Application of the essential work of fracture (EWF) concept for polymers, related blends and composites: A review

Bárány T., Czigány T., Karger-Kocsis J.

Application of the Essential Work of Fracture (EWF) Concept for Polymers, Related Blends and Composites: A Review

by

T. Bárány[1], T. Czigány[1], J. Karger-Kocsis[1,2]*

[1]Department of Polymer Engineering,
Faculty of Mechanical Engineering,
Budapest University of Technology and Economics,
H-1111 Budapest, Műegyetem rkp. 3., Hungary
[2]Department of Polymer Technology,
Faculty of Engineering and Built Environment
Tshwane University of Technology
Pretoria 0001, Republic of South Africa

* Author to whom correspondence should be addressed,
E-mail: karger@pt.bme.hu

Submitted to "Progress in Polymer Science", November, 2009 and revised March 2010

Abstract

The essential work of fracture (EWF) concept, originally developed by Broberg [1], became very popular to characterize the plane stress toughness of ductile polymers and related systems. The widespread use of the EWF is due to the simple specimens' preparation, easy testing and simple data reduction procedure. Though the EWF method is dominantly used for mode-I type loading, it has been successfully adopted for mode-II and mode-III type deformations, too. Moreover, attempts were also made to deduce plane strain toughness values from EWF tests. This paper critically reviews the application of the EWF to polymers, polymer blends and composites. The literature survey covers all major aspects of testing and related data reduction methods, and lists the EWF results achieved on different polymer systems. The latter were classified according to their synthesis/production and modifications. Special attention was paid to disclose the correlations between EWF and other fracture mechanical parameters, and to trace the EWF response to molecular and morphological parameters of the tested polymers.

Key-words: composites fracture mechanics, ductile fracture, polymers, essential work of fracture (EWF), energy partitioning, mode I, mode II, mode III

1. INTRODUCTION

Polymers, their blends and composites belong to the everyday life as they are widely used in different application fields. Their toughness is often a key property which can be determined by various standardized test methods. However, the toughness data of polymers can only be compared if the specimen preparation and testing conditions were exactly the same which is very seldom the case. By contrast, when adapting the fracture mechanical concept the inherent toughness of a given material can be determined. This seems to be essential to elucidate the structure-toughness relationships and to push forward the development of polymers.

Fracture mechanics aims at determining the response of a cracked material to applied load, and at offering methods to measure the toughness. The related approaches are grouped in linear elastic (plane strain conditions), elastic-plastic and post-yield fracture mechanics (plane stress conditions). Linear elastic fracture mechanics works for brittle systems that fail by catastrophic crack growth after reaching a threshold load (stress) value. The related criteria rely either on the stress field ahead of the crack tip (stress intensity factor or fracture toughness, K_c) or the energy release during crack extension (strain energy release rate or fracture energy, G_c). K_c and G_c find application to polymers undergoing brittle fracture in the related test. This prerequisite usually holds for thermosets and thermoset-based composites but not always applicable for thermoplastics.

For the toughness assessment of tough polymers the J-integral, the crack tip opening displacement (CTOD) and the essential work of fracture (EWF) methods are mostly used. The J-integral represents a

path-independent integral around the crack tip and thus considers also the plastic deformation at the crack tip. The critical value of the J-integral (J_c) is accompanied by full crack tip blunting prior to crack growth. J_c is usually deduced from the J resistance (J_R) curve when adopting the multiple specimen technique. This approach works well for not too ductile polymeric systems. The CTOD criterion is linked to the crack opening prior to its advance. However, this is seldom followed for polymers due to instrumentation problems. Instead of that usually the crack opening displacement (COD) is determined. The EWF approach is gaining acceptance to determine the toughness response of highly ductile polymers. The greatest advantage of EWF over the J-integral is that a clear distinction between surface (essential part) and volume-related (non-essential part) works is made. For a detailed description of the various fracture mechanical methods, testing standards, their applicability for polymer and polymer composites, the interested reader is addressed to valuable books (e.g. [2,3]).

The EWF approach became under spot of interest in the last decade. Therefore it is straightforward to summarize the achieved results, to draw the attention to the correct use of EWF, and to point out the unsolved problems. This survey is thus devoted to these aspects.

2. EWF CONCEPT

2.1. Theory

The EWF concept originates from Broberg's unified theory of fracture from the 70s [1,4-6].

Accordingly, stable crack growth is due to an increasing work input in an autonomous[1] inner region which is "filtered" through the gradually increasing action of the dissipative work in the neighbouring region. Thus the total work of fracture includes both the dissipative work in the outer "plastic" zone and the essential one in the inner autonomous zone. The latter is termed to fracture process zone and the essential work of fracture represents a material property (toughness). By contrast, the non-essential or "plastic" work is a geometry-depended parameter. The attribute "plastic" may suggest that in the outer fracture zone irreversible deformation takes place. This holds for thin, ductile metals, for which the EWF technique was originally developed [7] but not for polymers [8], as shown later. Pioneering role in the extension of the EWF to polymers should be assigned to Mai and coworkers [6,9,10].

As coined above the total work of fracture (W_f) can be partitioned into two components; i) the essential work of fracture (W_e) consumed in the inner fracture process zone to create new surface, and ii) the non-essential (or plastic) work (W_p) performed in the outer "plastic" deformation zone – see Figure 1.

[1]Wording of Broberg

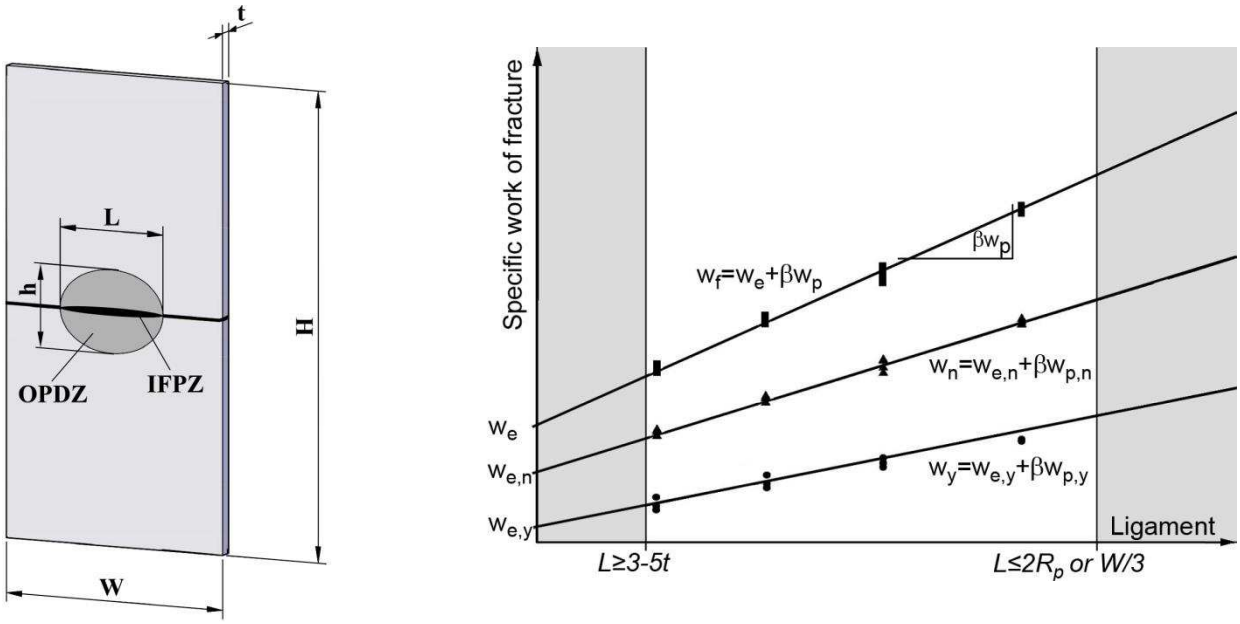

Figure 1 Schematic diagram showing the fracture zones (a) (IFPZ: inner fracture process zone, OPDZ: outer process dissipation zone) and the data reduction method of the EWF (b)

The total work of fracture (W_f), calculated from the area of the force-displacement (F-x) curves (see Figure 1b) is composed of Equation (1):

$$W_f = W_e + W_p \tag{1}$$

Assuming that both zones are within the ligament of the specimen (cf. Figure 1a), Equation 1 can be rewritten into the specific terms (Equations (2) and (3)):

$$W_f = w_e \cdot Lt + \beta w_p \cdot L^2 t \tag{2}$$

$$w_f = w_e + \beta w_p \cdot L \tag{3}$$

where L is the ligament length, t is the specimen thickness and β is the shape factor related to the form of the outer plastic dissipation zone. Accordingly w_e is surface-, whereas w_p is volume-related. Equation 3 is the base of the data reduction: the specific work of fracture data determined on specimens with varying ligaments are plotted as a function of the ligament length. w_e is given by the y(w_f)-intercept of the related linear regression. From the slope (βw_p) of the linear regression w_p can be explicitly deduced for some shapes of the outer plastic zone. The β parameter for circular, elliptical and diamond-type zones are $\pi/4$, πh/4L, and h/2L (e.g. [6]), respectively, where h is the height of the corresponding zone (cf. Figure 1a). Note that in the outer plastic dissipation zone crazing, voiding (continuity/discontinuity-type events), shear deformation (isotropy/anisotropy-type events) and their combination may occur.

2.2. Testing and standardization

There are some requirements that should be met before the EWF method is applied to assess the toughness [6]:

- full ligament yielding prior to crack initiation

- self-similar load-displacement curves, i.e. the load-(load line) displacement curves of the specimens registered at different ligament lengths can be "unified" (covering each other) by linear transformation
- plane stress condition prevails and the volume of the outer plastic dissipation zone is scaled with the square of the ligament (meaning that Equation 3 holds)

Though complete ligament yielding should precede the onset of crack initiation, this requirement is rarely fulfilled. Note that full ligament yielding must show a load drop in the related F-x curves. The yielding-caused load drop may be instantaneous or may exhibit some time dependence. Karger-Kocsis [11,12] argued that the best EWF "model materials" are amorphous polymers prone for shear yielding.

Nonetheless, the overwhelming majority of the EWF studies was related to polymeric systems in which ligament yielding and crack initiation/growth were superposed to one another.

By contrast to the above ligament yielding criterion, attention was always paid to the "self-similarity" of the F-x curves taken at different ligaments. Based on the large body of EWF works published (see later) one can get the impression that the fulfilment of this criterion is the only ("sine qua non") prerequisite of the EWF application. Note only that similar F-x curves can be obtained when the ligament yielding occurs simultaneously with crack growth. It has to be underlined that without a clear indication for ligament yielding in the corresponding F-x curves, the EWF preconditions are not fully met. Therefore the related EWF parameter can hardly represent the inherent material toughness but a toughness value for comparison purpose. Nevertheless, the related data are well suited for further toughness-oriented material development. In order to meet the plane-stress conditions of the specimens their ligament range is limited. For the lower bound usually $L \geq (3 \ldots 5)t$, whereas for the upper one $L < 2r_p$ or W/3, where r_p is the radius of the plastic zone (see Equation (4)) and W is the width of the (deeply) double edge notched tensile ((D)DEN-T) specimens, are considered. The restriction W/3 is imposed to prevent edge effects.

$$2r_p = \frac{1}{\pi}\left(\frac{Ew_e}{\sigma_y^2}\right) \qquad (4)$$

where E is the Young's modulus and σ_y is the uniaxial tensile yield stress of the material.

Note that $2r_p = L$ means that the ligament of the DEN-T specimen really yields prior to crack initiation. The criterion $L \leq 2r_p$ or W/3 means that the most restrictive one of them should be considered.

Though they are reasonable size criteria, they do not have excluding character from the viewpoint of the applicability of the EWF. For amorphous copolyesters for example both lower and upper bounds proved to be too restrictive as documented in Refs. ([8,12] and references therein).

An alternative criterion for pure plane stress conditions is given by the Hill criterion [13]. Based on this the maximum net section stress (σ_n) calculated by dividing the maximum load with the ligament cross section, should be independent of the ligament and show a constant value $m\sigma_y$, where m is the plastic flow

constraint factor. m=1 for single edge notched tensile (SEN-T) and 1.15 for DEN-T specimen. In the mixed mode (plane stress/plane strain) region σ_n increases with decreasing ligament length and thus the related data do not represent valid EWF measurements.

When w_e is an inherent material parameter then it should be independent of the specimen's geometry. Mai and Cotterel [14] verified this first by using different specimen configurations. Nonetheless, under mode I deformation (crack tip opening) SEN-T, DEN-T and single edge notched bending (SEN-B especially) specimens are almost exclusively used for EWF testing. This can be attributed to the following issues: i) rather easy specimen preparation, ii) wide acceptance of Charpy tests performed on SEN-B specimens, and iii) few problems during testing of the above mentioned specimens (no buckling, wrinkling, and the like causing dissimilarities in the F-x curves).

2.2.1. Specimens and their criteria

A large body of experimental works was devoted to the effects of the specimen size (width, clamping length etc.), ligament assessment (before and after fracture), monitoring of the deformation (crosshead movement, videoextensometer), procedure and methodology of notching on the EWF parameters. It was found that with increasing specimen size the correlation coefficient of the linear regression increases. The ligament assessment (prior to the test or post mortem) had a marginal effect on the regression parameter (mean values and standard deviation) [15]. Measuring the load line displacement by videoextensometer resulted in slightly lower βw_p values whereas the mean w_e remained unaffected [15,16]. This was attributed to the viscoelastic nature of the specimen. It turned out, however, that the notching procedure and thus the corresponding notch tip radius may strongly influence the mean w_e values without affecting the βw_p markedly [15,17]. With decreasing notch tip radius the mean w_e was reduced. Note that in the work of Pegoretti et al. [17] and Martinez et al. [15] as radii less than 20 and 5 μm, respectively, were given. It is noteworthy that in the recommendation of Williams and Rink [18] for the notch tip radius ≤15 μm was given. Martinez et al. [15] observed almost a doubling in the w_e values when notching occurred by a femtolaser beam or a traditionally by a razor blade (with or without diamond coating of the blade). The exceptional large difference in the corresponding mean w_e values was traced to the assumption whether the crack growth started in a non-deformed (femtolaser cut) or in an already deformed (by blunting) ligament area. Though the above information is relevant, the reproducibility of the EWF, at least when using the same type of notching, should not be questioned. It has to be pinpointed that the cited works were performed on linear low density polyethylene (LLDPE) [17] and poly(propylene-block-ethylene) copolymer (PP-BC) [15], respectively. Both of them are "EWF problematic" (disclosed later) semicrystalline polymers. To clarify the effects of the "notchology", the authord recommend to perform EWF tests on suited "model polymers" (amorphous copolyesters). This is the right place to call the attention to a fundamental question: should be a method universally applicable under proper experimental conditions or not? Of course, yes, however, "proper EWF conditions" for many polymers do not exist at

ambient temperatures where most of the tests are done. On the other hand, these conditions are met by amorphous copolyesters always at room temperature (RT).

Almost exclusively linear regression is adapted to the w_f-L point pairs measured in accordance with Equation 3. However, based on the analogy between the EWF and J-integral determination (both of them represent crack resistance behaviour as disclosed later) it was also recommended to fit the experimental w_f – L data by a power law function [19-21].

The authors of the review are sure that the power law data reduction will hardly be accepted by the EWF community.

2.2.2. Energy partitioning

Though the EWF is already based on energy partitioning concept (i.e. distinction between essential and non-essential work of fracture), further energy-based distinguishing criteria have been introduced. Mai and Cotterell [9] defined a crack initiation-related (observed visually) component whereby the elastically stored in the specimen was taken into account. Based on the load drop at full ligament yielding in the F-x curves another partitioning was recommended that disregarded the portion of the elastic energy [12]. The above two concepts, well accepted in the EWF literature, are depicted schematically in Figure 2.

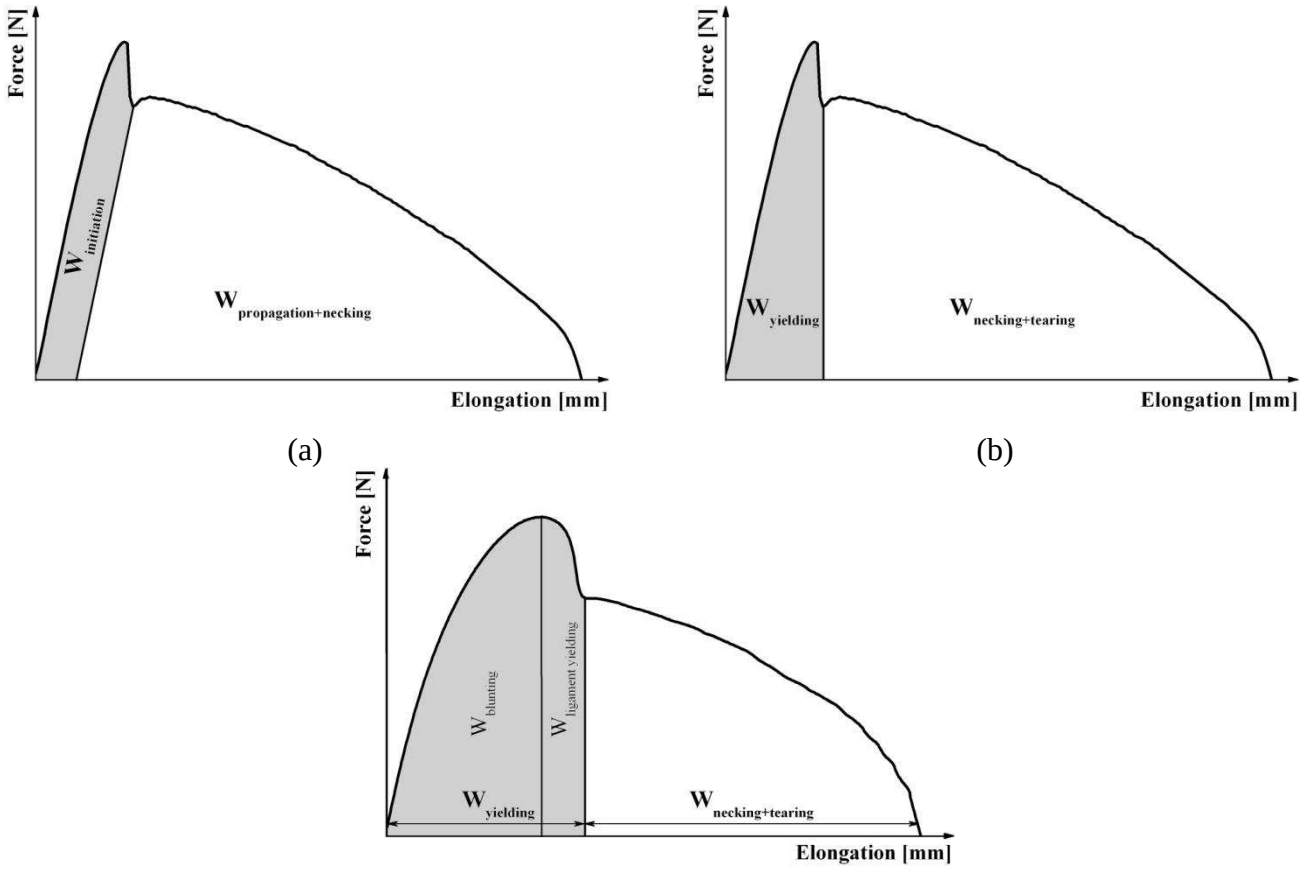

Figure 2 Energy partitioning according to the initiation (a) and yielding concepts (b, c), schematically. Note: in case b) the ligament yielding is instantaneous, whereas in case c) time-dependent.

Note that the partitioning of the F-x curves differs from one another only how the elastically stored energy is considered. According to the "initiation" concept it is supposed that the elastic contribution is released during the subsequent fracture process.

The mathematical treatise of both energy partitioning methods is identical (Equations (5) and (6)):

$$w_f = w_{f,y} + w_{f,n} = \left(w_{e,y} + \beta w_{p,y} \cdot L\right) + \left(w_{e,n} + \beta w_{p,n} \cdot L\right) \quad (5)$$

$$w_f = w_{f,I} + w_{f,II} = \left(w_{e,I} + \beta w_{p,I} \cdot L\right) + \left(w_{e,II} + \beta w_{p,II} \cdot L\right) \quad (6)$$

For some polymers, showing delayed yielding (not instantaneous), the yielding section can be split further into crack blunting and ligament yielding [22]. The related partitioning is shown schematically in Figure 2c.

The above energy partitioning was pushed forward by two aspects: i) to trace the EWF parameters to (super)molecular characteristics of the corresponding polymer, and ii) to derive a plane-strain EWF value. This is the topic of the last section (Unsolved issues) of this contribution. Recently, a very good review paper [23] appeared which lists many aspects of the EWF testing (specimen geometry and testing, shape factor determination, energy partitioning, extension for mode III tearing etc.).

2.2.3. Limitation of the EWF use

The EWF approach has been criticized as useless since the w_f vs. L data pairs may result in a negative intercept (w_e) or negative slope (βw_p) (e.g. [24]). The reason behind this behaviour is always a change in the stress state (plane stress-plane strain) and/or in the failure mode (ductile-brittle) of the specimens during loading. In some cases, however, the above disclosed energy partitioning is the right tool to overcome the problems. It was shown that amorphous poly(ethylene naphthalate) (PEN) of low mean molecular mass exhibits unstable fracture in the necking+tearing stage (cf. Figure 3).

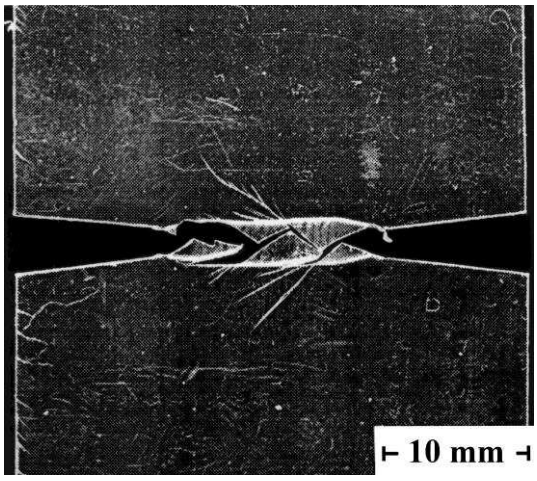

Figure 3 Unstable cracking after full ligament yielding in a DEN-T specimen from low molecular weight PEN [25] (Reprinted from: Karger-Kocsis J., Moskala E. J.: Molecular dependence of the essential and non-essential work of fracture of amorphous films of poly(ethylene-2,6-naphthalate) (PEN). Polymer, **41**, 6301-6310 (2000), Copyright 2000, with permission from Elsevier)

This unstable cracking resulted in a negative βw_p value (being "nonsense") when the w_f vs. L data were considered (Figure 4a). On the other hand, the related curves were "self-similar" until the instantaneous yielding (Figure 4b). Therefore, the yielding-related essential ($w_{e,y}$) and yielding-related non-essential ($\beta w_{p,y}$) parameters could be determined accordingly.

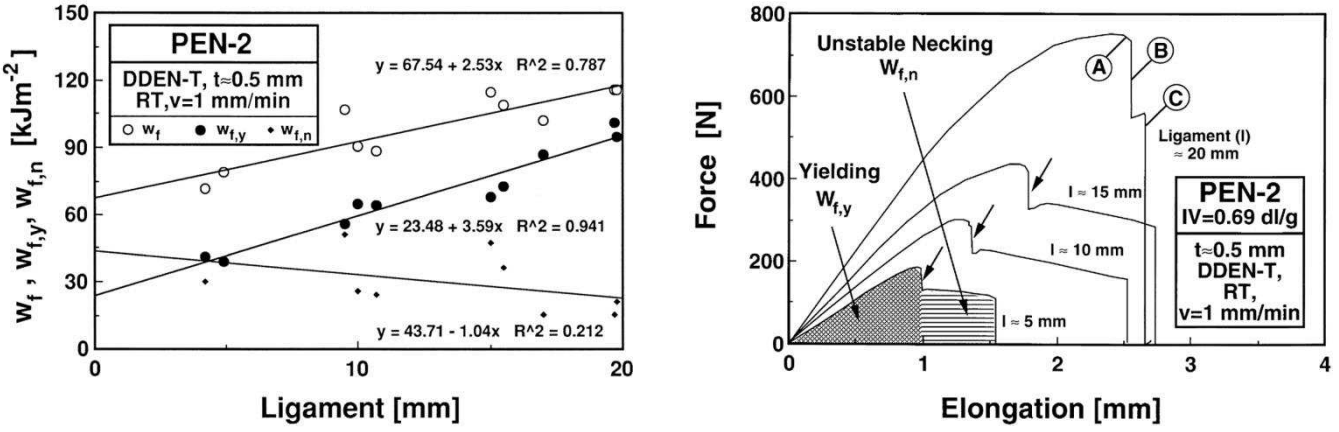

(a) (b)

Figure 4 Data reduction of the EWF tests performed on amorphous PEN of low molecular mass (a) and the related primary load-displacement (F-x) curves measured on DEN-T specimens (b) [25] (Reprinted from: Karger-Kocsis J., Moskala E. J.: Molecular dependence of the essential and non-essential work of fracture of amorphous films of poly(ethylene-2,6-naphthalate) (PEN). Polymer, 41, 6301-6310 (2000), Copyright 2000, with permission from Elsevier)

Another approach tried to consider the ductilely failed proportion of the fracture surface of DEN-T specimens which underwent ductile-brittle fracture transition during loading. In this case the ductile/brittle ratio was determined post mortem by microscopic inspection [26]. Martinez et al. [23] proposed another approach by defining the ductility level (displacement at rupture in respect to the initial ligament length). Attention was paid also to the accurate determination of the lower L threshold separating the mixed mode state from the plane-stress one (e.g. [27])

The EWF has a strict limitation: it can hardly be adapted for polymers in which the ligament yielding is accompanied with work (stress or strain) hardening. Here, it does not grow from the notch, i.e. transverse to the loading direction, as expected. Instead of that the crack "deflects" along the loading direction without advancing. Simultaneously, a prominent work hardening (in that case strain hardening) occurs (cf. Figure 5). This is very similar to a neck formation usually observed in uniaxial tensile tests.

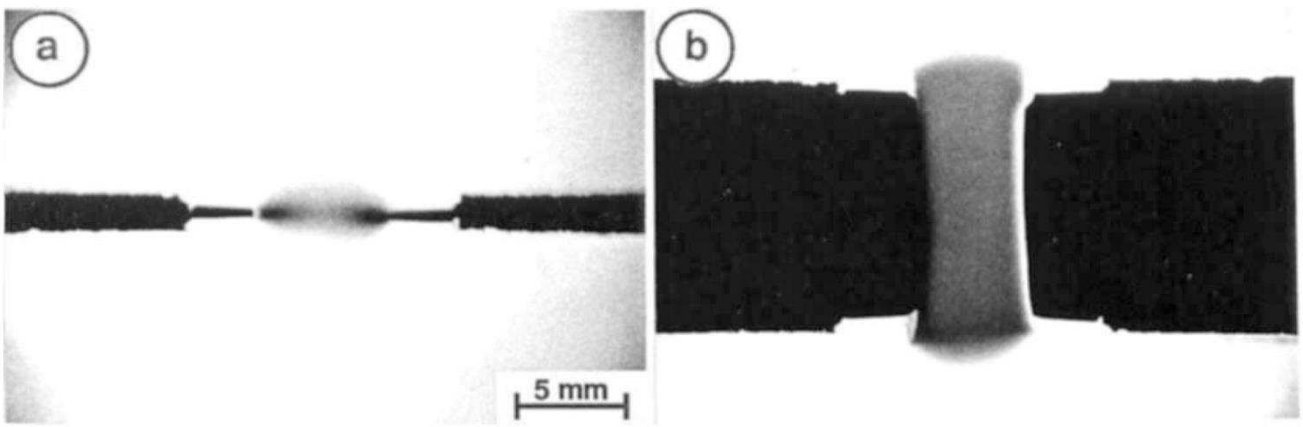

Figure 5 Light microscopic pictures (back illumination) showing the outer plastic zone (a) and the strain hardening of the ligament (b) caused by the injection moulding-induced skin-core structure. Note: the latter was oriented along the loading direction [28] (Reprinted from: Karger-Kocsis J., Mouzakis D. E.: Effects of injection molding-induced morphology on the work of fracture parameters in rubber-toughened polypropylenes. Polymer Engineering and Science, 39, 1365-1374 (1999), Copyright 1999, with permission from John Wiley and Sons)

This crack deflection can be considered as caused by the Cook-Gordon mechanism [29]. Note that its onset is favoured by the inherent anisotropic (super)molecular structure of the tested material. Such structure develops in uniaxial oriented films, in injection moulded parts showing prominent skin-shear-core structure (cf. Fig. 5), composites with various reinforcements aligned in the loading direction (e.g. microfibrillar composites, MFC) and the like. It has to be underlined that the above problems in neat polymers appear exclusively in semicrystalline ones (mostly produced by polymerization and thus having high molecular weights) which are prone for deformation (strain)-induced changes in the morphology. Under morphology changes alterations in the crystalline superstructure (orientation and defolding of the lamellae), polymorphic transitions (transition from one crystalline form to another), molecular alignment in the amorphous phase etc. are meant.

2.2.4. Standardization

The EWF method became very popular for the assessment of the plane-stress fracture toughness of thin polymer sheets. In spite of that fact that it use has some prerequisites, the related criteria seem to be sometimes flexible enough. The test conditions (loading rate, gauge length, temperature etc.) are selected freely by the researchers. In order to make the EWF results comparable the testing conditions should be fixed, i.e. standardization is required. This has been early recognized and the stage of the standardization procedure is summarized below.

At first, Clutton has summarized the results of a series of round-robin exercises (between 1992 and 1999) under the guidance of the ESIS TC4 Committee [30]. In this protocol it was concluded that the specimen size (length, width) does not influence the results, and for the loading rate 0.2 times of the gauge length in mm/min was calculated. The shape of the formed plastic zone is much more difficult to measure in case

of plastics than metals. The protocol highlights the importance of the self-similarity of load-displacement curves, the sensitivity of the method to notching methodology, and emphasizes to consider the lower bound of the ligament lengths (3t, 5 mm).

Later on Williams and Rink have summarized the results of two round-robin test series performed by the ESIS TC4 group [18]. The selected material was an ethylene/propylene copolymer film having 100 μm nominal thickness. This report pinpointed some uncertainty due to differences in the notching methodology. Therefore it was recommended to give the maximum standard error (in this case S=3 kJ/m^2) or minimum correlation coefficient (in this case R^2=0.98).

Simultaneously these round-robin test series an ISO standardization process – ISO/CD 18874 – took place. This draft [31,32] includes all details of the EWF method: specimen shape and dimensions, specimen preparation, testing parameters, notch types and dimensions, evaluation of test results and stress criteria etc. This is now under review, especially due to poor reproducibility of the results achieved in round robin tests. It worth to note that each protocol recommend to use DEN-T specimens and the round-robin tests coordinated by ESIS TC4 Committee have used mainly polyolefins which are not the best 'model' material for EWF tests at RT. Interested reader may get information on the present stage of the ISO standard draft at the web site in Ref. [31].

This is the right place to give some guide-lines on the specimens and their testing. DEN-T configuration (thickness< 2 mm, width>30 mm, gripped /gauge/ length>30 mm) is preferred as plane stress condition prevail owing to the colinear notches in this specimen cut from thin films and sheets. Though the notching is topic of intensive disputes, razor blade cut is usually fine. The DEN-T specimens – under static conditions – are usually loaded with a deformation rate less than 20 mm/min. Recall that the above ISO draft gives a deformation rate value in function of the specimen gauge length. The ligament range for valid EWF tests was well disclosed before. Note that for some polymers the limitation for the ligament range may be too strict.

3. EWF UNDER MODE I-TYPE LOADING

As quoted before the majority of EWF measurements were performed under mode I loading. In addition, the EWF concept was mostly adapted for quasistatic (i.e. low strain rate, low 'loading frequency') and in lesser extent in dynamic (impact; high strain rate, high "loading frequency") tests. In order to support the overview, the published results below are grouped into those achieved in static and dynamic tests, respectively, on polymers, polymer blends and composites. Grouping into static and dynamic loadings is reasoned by the fact that polymers exhibit "frequency embrittlement", i.e. they become less under impact conditions. As a consequence, the conditions (including the suitable materials) of valid EWF tests are markedly different from the static ones. In addition, many groups were working on the static, while only few dealt with dynamic EWF measurements.

3.1. Static loading

The results discussed below are mostly performed at a loading rate of less than 100 mm/min. In order to support the overlook the EWF results are tabulated. The corresponding tables contain also information on the specimen size and testing configuration. The comments reflect the major findings of the cited papers according to the authors' judgement.

To support the overlook the EWF results are listed according to a grouping which considers the synthesis/manufacturing (polymerization – Table 1, polycondenzation – Table 2, polyaddition – Table 3, crosslinking – Table 4, natural polymers (biopolymers) – Table 5), and compositions (blends – Table 6, micro- and macrocomposites – Table 7, nanostructured, nanoreinforced systems – Table 8) of the EWF studied polymer systems.

Table 1 EWF results on polymerization polymers under static loading

Material	Specimen type	Testing conditions		EWF parameters		Comments	Literature
		T [ºC]	v [mm/min]	w_e [kJ/m^2]	βw_p [MJ/m^3]		
LDPE	DEN-T	-25…+30	10	~11	7-9	Annealing/quenching effects, w_e via COD estimated	[33]
LLDPE	DEN-T	-25…+30	10	18-25	13-19	Annealing/quenching effects, w_e via COD estimated	[33]
LLDPE	DEN-T	25	5	19-27	7-14	Effects of nucleation agents; energy partitioning	[34]
LLDPE	SEN-T, DEN-T	RT	10	47-100	20-31	Effects of specimen width and LLDPE types	[35]
LLDPE	DEN-T	RT	20	47	9	Plane strain w_e estimated	[36]
LLDPE	DEN-T	RT	100	36-39	~9	Effects of notching, reproducibility	[17]
LLDPE	DEN-T	RT	2	4-34	9-70	Effects of orientation in drawn tapes	[37]
HDPE	SEN-T, DEN-T	RT	10	61	37	Effect of specimen type	[35]
HDPE	SEN-T, DEN-T	20	10	78-149	7-19	Effects of HDPE types; comparison with the J-integral	[9]
HDPE	DEN-T, CN-T	20	0.5	35-36	42-56	Comparison with the J-integral	[10]
HDPE	DEN-T	RT	5	21-38	6-11	Effects of HDPE grades	[38]
HDPE	DEN-T	RT	5	50-76	10	Effects of orientation; energy partitioning	[39]
PP-H	DEN-T	RT	2-100	49-52	9-10	Effects of specimen height and deformation rate; mixed-mode EWF results; energy partitioning	[40]
PP-H	DEN-T	23	2	244	36	Effects of orientation; high values due to crack deflection (Cook-Gordon mechanism)	[41]
PP-BC	DEN-T	23	2	19-276	5-28		
PP-H	SEN-T	RT	2.5	17-43	11-40	Effect of orientation; w_e reduced by increasing v	[42]
PP-H	DEN-T	RT	2	~9	~8	Effects of annealing; comparison with tensile impact	[43]
PP-H	DEN-T	RT	5	~55	2-4	Thermal oxidation reduced only the βw_p term	[44]
PP-H	DEN-T	0-100	5	30-60	2-10	w_e drops between two plateau values at T=60ºC, βw_p goes through a maximum; strong MW effect	[45]
PP-H	DEN-T	RT	10	6-14	0.5-14	Effects of draw ratio and draw direction	[46]

PP-H	DEN-T	RT	$6 \cdot 10^4$	10-45	0-22	Effects of deformation rate (covering dynamic range); energy partitioning	[47]
PP-H, PP-BC	DEN-T	-40-+70	2	20-80	4-14	Effects of PP type, annealing/quenching, testing temperature; fractography	[48-50]
PP-H	DEN-T	RT	2-100	45-58	9-10	Effects of specimen dimension and preparation	[51]
PP-H (beta)	DEN-T	not disclosed	not disclosed	0.5-31	0.1-9	Effects of quenching and specimen preparation	[52]
PP-H (alpha, beta)	SEN-B	RT	500	1-7	~0	"Near" plane strain w_e; βw_p increased with beta-content	[53]
PP-H (alpha, beta)	SEN-T	RT	5	34	7-20	Beta-content enhances the βw_p only	[54]
PP-H (alpha, beta)	DEN-T	RT	5	32	3-10	Phase transformation toughening proposed; beta-content affects the βw_p term	[55]
PP-H (alpha, beta)	DEN-T	RT	2	7-16	6-13	Effects of annealing (beta-alpha transition); annealing decreased both w_e and βw_p	[56]
PP-BC	DEN-T	23	5	21-31	10-21	Effects of molecular weight (controlled rheology); w_e increased linearly with M_n, βw_p decreased with increasing M_z	[57]
PP-BC	DEN-T	23	5	12-41	6-19	Annealing increased w_e and decreased βw_p; w_e via COD estimated.	[58]
PP-H, PP-BC	DEN-T	23	2	16-77	2-14	Effects of injection moulding induced morphology (orientation), thickness, copolymer content	[59]
PP-H, PP-BC	DEN-T	RT	2	6-210	1-18	Effects of processing methods, orientation, thickness; attempts to correlate EWF with morphological parameters	[60,61]
PP-BC (alpha, beta)	DEN-T	25	5	30-40	7-10	Effects of crystallinity and beta-content	[62]
Elastomeric PP	DEN-T	23	1	8-20	9-54	Effects of MW; Mode I and Mode III (trousers) loading	[63]

Elastomeric PP (iPP/aPP block copolymer)	DEN-T	RT	1	8-20	5-11	Morphology dependence	[64]
sPP	DEN-T	1	1-100	24-29	3-6	Effects of MW, crystallinity, deformation rate Energy partitioning, delayed necking	[22]
sPP	DEN-T	RT	1	27-30	~4	Effects of crystallinity and UV aging, energy partitioning	[65]
poly(propylene carbonate)	DEN-T	20	1	9-12	2-12	Effects of MW; plastic zone recovery at RT	[66,67]
poly(cyclo olefin)	DEN-T	15-163	1	7-12	~3	Effects of temperature; energy partitioning; both w_e and βw_p passed a maximum as a function of temperature; w_e via COD estimated; molecular orientation measured in situ	[68]
HIPS	SEN-T, DEN-T	20	10	1.1	-	Plane strain value	[9]
HIPS	SEN-T, DEN-T	25-80	1-50	5-8	0.2-0.8	Effects of specimen size, orientation, temperature; w_e via COD estimated	[69]
ABS	SEN-B	20-80	2	3-6	0.6-1.2	Plane strain value	[70]
uPVC	DEN-T	22	1	3-11	3-4	Specimens from pipe; w_e the higher, the higher the “processing level” is	[71]
uPVC	DEN-T	RT	1	2-30	5-6	Effects of pipe and specimen orientation; pipe orientation increased w_e markedly	[72]
uPVC	DEN-T	RT	12	12-50	-	Effects of thickness and ligament; comparison with J integral	[73]
uPVC	SEN-T, DEN-T	23-60	2-50	35-43	3-4	Effects of specimen size, deformation rate and temperature; energy partitioning	[74]
uPVC	DEN-T	23-60	5	21-40	2-4	Effects of specimen thickness and temperature; w_e via COD estimated	[75]
uPVC	DEN-T	RT	1-100	18-23	2-3	Effects of specimen thickness; energy partitioning; methods compared	[76]
PVDF	DEN-T	23	1	34-48	4-9	Effects of specimen thickness and annealing; change in the morphology detected; COD measured	[77,78]

POM	DEN-T	80-100	0.002-2	7-50	0.2-13	Effects of MW and deformation rate	[79]

Table 2 EWF results on polycondenzation polymers under static loading

Material	Specimen type	Testing conditions		EWF parameters		Comments	Literature
		T [°C]	v [mm/min]	w_e [kJ/m^2]	βw_p [MJ/m^3]		
PA-6	DEN-T	RT	5-500	2-65	3-21	Effects of thickness, processing (injection/compression moulding) and testing (notching) conditions	[80]
PA-66	SEN-T, DEN-T	RT	10	29-52	7-15	Effect of specimen width and PA-66 type	[35]
PA-66	SEN-T, DEN-T	RT	10	48-51	7-8	Energy partitioning; comparison with J-integral	[9]
PA-66	DEN-T	RT	1-500	11-26	1-14	Energy partitioning; effect of humidity and deformation rate	[81]
PET	DEN-T	RT	5	35	~2	Effect of annealing; for w_f vs. L power law description proposed; w_e via COD estimated	[19]
PET (semicrystalline)	SEN-T, DEN-T	23-140	2-50	57-70	8-18	Effects of specimen type, dimensions, deformation rate and temperature; w_e via COD estimated; J-integral with w_e compared	[82]
PET (semicrystalline)	DEN-T	23-160	5	58-74	4-17	Both w_e and βw_p went through a maximum as a function of T	[83]
PET (semicrystalline)	DEN-T	23-140	5	52-75	5-17	Effect of temperature on w_e and βw_p	[84]
PET (biaxial oriented)	DEN-T	RT	2	53-68	6-9	For mixed mode (plane stress-plane strain) data by linear regression proposed	[85]
PET (biaxial oriented)	DEN-T	RT	2	46-66	6-9	Effects of orientation and thickness	[86]
PET (biaxial oriented)	DEN-T	-20-40	1-100	85-190	1-9	Limitations of EWF discussed	[87]
PET (biaxial oriented)	DEN-T	25-160	5	34-46	2-16	Effects of orientation and thickness; βw_p maximum at T_g	[88]

PET (biaxial oriented, filled)	DEN-T	RT	1-20	54	9-15	Effect of orientation; Mode III – w_e determined	[89]
PET (amorphous)	SEN-T, DEN-T, CNT	RT	10	52-56	12-29	Effect of specimen type	[35]
PET (amorphous)	DEN-T	23-70	5	80-82	10-11	Energy partitioning; COD determined and w_e via COD estimated	[90]
PET (amorphous)	DEN-T	-20-60	2	6-77	10-13	Energy partitioning; hygrothermal aging	[91]
PET (amorphous)	DEN-T	RT	1	35	11	Comparison with other polyesters	[92]
PET (amorphous)	DEN-T	RT	2	49-53	~10	Energy partitioning; physical and thermal aging; correlation with enthalpy relaxation (also Mode III testing in Ref. 85)	[93,94]
PETG				39-43	6-8		
PETG	DEN-T	RT	0.1-50	22-34	~8	Effect of clamping length	[95]
PETG	DEN-T	RT	1	30	~8	Energy partitioning introduced; EWF “model material” recommended	[12]
PETG	DEN-T	RT	2.54	20-33	5-6	Effect of hygrothermal aging in different fluids	[96]
PETG	DEN-T	RT	1	10-22	9-10	Effects of specimen dimension and notching; theoretical and measured values compared	[97]
PETG (antiplasticized)	DEN-T	RT	2-100	20-51	6-9	Effects of antiplasticizer amount and physical aging	[98]
PCTG	DEN-T	RT	1-100	33-36	5-7	Energy partitioning; effect of deformation rate	[99]
PCTG	DEN-T	RT	1	36-39	5-8	w_e is thickness independent (t=0.5-6 mm)	[100]
Copolyesters	DEN-T	RT	0.6	15-35	not reported	Aging (physical, hygrothermal) effects; w_e and drop weight impact results collated	[101]
Copolyesters (also bilayers)	DEN-T	RT	1	30-46	not reported	Energy partitioning; COD determined and w_e via COD estimated	[102]
Copolyesters (amorphous)	DEN-T	RT	1	30-44	not reported	Energy partitioning; $w_{e,y}$ was independent on the MW	[103]
Copolyesters (amorphous)	DEN-T	RT	1-1000	35-65	6-12	w_e was reduced or went through a minimum as a function of deformation rate – the latter was accompanied with strain-induced crystallization	[104]

PBT	DEN-T	25-100	5	27-33	3-4	Energy partitioning	[105]
PBT	SEN-T	24	2-50	36-41	3-4	Effect of thickness	[106]
PBT	SEN-T, DEN-T	24	5	36-37	3-4	Effects of specimen types, thickness and width	[107]
PBT (semicrystalline)	SEN-T, DEN-T	23-100	5	26-36	3-7	Effects of thickness, orientation, specimen dimension and temperature	[108]
PBT (semicrystalline)	DEN-T	23-100	5	25-27	~3	Effect of temperature on w_e and βw_p	[84]
PBT (semicrystalline)	DEN-T	RT	1	31	12	-	[92]
PPT (semicrystalline)	DEN-T	RT	1	41	9	-	[92]
PEN	DEN-T	RT	2	56	3	Power law for w_f vs. L considered	[85]
PEN (semicrystalline)	DEN-T	23-140	5	54-75	5-23	Effect of temperature on w_e and βw_p	[84]
PEN (semicrystalline)	SEN-T, DEN-T	23-140	2-50	55-75	5-23	Effects of deformation rate and temperature; w_e via COD estimated; comparison with J-integral	[109]
PEN (amorphous)	DEN-T	RT	1	42-67	9-10	Energy partitioning; effect of MW; plain strain value proposed; w_e via COD computed	[25]
PEN (amorphous)	DEN-T	RT	1-100	43	9-11	Energy partitioning; strain rate - molecular weight correlation; w_e via COD computed	[110]
Polyester elastomer	DEN-T	RT	2	100-105	~16	Mixed mode data; alternative method to determine β	[111]
Polyester elastomer	DEN-T (trousers tear)	23	50	34-71	5-13	Effects of hard segment content, specimen orientation; energy partitioning; curved crack during tear	[112]
PC	SEN-T, DEN-T	RT	1	29-43	2-4	Effects of specimen type and thickness	[113]
PC	SEN-T	25-100	2-50	30-34	3-6	w_e independent of both temperature and deformation rate	[114]
PC	SEN-T, DEN-T	25-120	5	39-46	2-6	Effect of temperature; energy partitioning; SEN-T data higher than DEN-T data	[115]

PC	DEN-T	RT	10	18-48	4-8	Effect of physical (heat) aging; results compared with strain energy density and energy release rate – contradictory results	[116]
PC	SEN-T, DEN-T	RT	1	25-35	3-4	Effects of orientation, notching; comparison with J-integral; plane strain w_e deduced and comfirmed	[117]
PEEK (semicrystalline)	DEN-T	20	1	20-51	3-12	Effect of temperature; energy partitioning; w_e via COD computed	[118,119]
PEEK (semicrystalline, amorphous)	SEN-T	RT	1	54-65	4-10	w_e via COD computed	[120]
PEEK (semicrystalline)	DEN-T	23-140	5	32-38	5-8	Effects of orientation and thickness; mode III tear determined	[121]
PI	SEN-T, DEN-T	RT	2-20	39-43	1.2-3.7	Effects of PI type and deformation rate	[35]
PEI, PI	DEN-T	RT	2	37-57	3-4	Power law for w_f vs. L considered	[85]

Table 3 EWF results on polyaddition polymers under static loading

Material	**Specimen type**	**Testing conditions**		**EWF parameters**		**Comments**	**Literature**
		T [ºC]	**v [mm/min]**	**w_e [kJ/m^2]**	**βw_p [MJ/m^3]**		
PU (thermoplastic)	DEN-T	RT	5	25-48	2-5	Dependence on network (structural) properties; w_e vs. M_c relationship proposed	[122,123]

Table 4 EWF results on crosslinked polymers under static loading

Material	**Specimen type**	**Testing conditions**		**EWF parameters**		**Comments**	**Literature**
		T [ºC]	**v [mm/min]**	**w_e [kJ/m^2]**	**βw_p [MJ/m^3]**		
PE	DEN-T	80, 110	0.05-100	7-20	0.5-13	Both w_e and βw_p decrease with increasing crosslink density; effect of deformation rate	[124]
TDV (PP/EPDM)	CN-T, DEN-T	RT	25.5	54	~4	Comparison with J-integral	[125]

TDV (PP/EPDM)	DEN-T	20	5	25-34	10-14	With increasing EPDM content and its crosslink density both w_e and βw_p increased	[126]
TDV (beta PP/EPDM)	DEN-T	25	5	16-25	9-11	Beta-phase content of PP improved w_e	[127]
TDV (PP/SBS) (PP/SBS-crosslinked)	DEN-T	RT	10	8-15	2-7	w_e increased and w_p decreased with rubber content	[128]
EP	DEN-T	RT	0.5	6-18	0.1-1	Attempts to correlate w_e with T_g and yield stress	[129]
EP	SEN-B	RT	0.05	<2	<0.5	-	[130]
EP (flexibilized, filled)	SEN-T	RT	0.5	2-25	<0.5	w_e decreased with increasing pigment content of the paint composition	[131]
Polypeptides	DEN-T	RT(water)	3	<0.2	-	Attempt to extend the EWF for hydrogels	[132]

Table 5 EWF results on natural polymers (biopolymers) under static loading

Material	**Specimen type**	**Testing conditions**		**EWF parameters**		**Comments**	**Literature**
		T [ºC]	**v [mm/min]**	**w_e [kJ/m^2]**	**βw_p [MJ/m^3]**		
Starch (plasticized)	DEN-T	RT(humidity)	5	3-11	0.6-5	Effect of humidity; w_e with strain energy release rate compared	[133]
Cellulose (functionalized)	DEN-T	RT(humidity)	2	1-6	0.2-0.9	Effect of humidity; w_e via COD computed	[134]
Gelatin/maltodextrin	DEN-T	RT	50	~0.1	~0.003	w_e via COD computed	[135]

Table 6 EWF results on polymer blends under static loading

Material	**Specimen type**	**Testing conditions**		**EWF parameters**		**Comments**	**Literature**
		T [ºC]	**v [mm/min]**	**w_e [kJ/m^2]**	**βw_p [MJ/m^3]**		
LDPE/LLDPE (20/80 wt%)	DEN-T	-25-+30	10	20-22	12-15	Effect of annealing/quenching; w_e via COD estimated	[33]
LLDPE/PP	DEN-T	RT	2	10-34	-	Results on microfibrillar (PP) and isotropic	[136]

(15, 30 wt%)						specimens; w_e correlated with the strain-hardening modulus	
LDPE/EVA (5 wt%)	DEN-T	RT	10	8-38	4-14	Effects of orientation and photooxidation; energy partitioning	[137]
HDPE/PP/SEBS (80/10/10 wt%)	SEN-T, DEN-T	22	1-100	22-58	17-30	Effects of specimen size, specimen dimension and deformation rate; w_e of SEN-T much higher than DEN-T	[138]
HDPE/POE (5, 10 wt%)	DEN-T	RT	5	8-60	1-21	Strong orientation effect	[139]
PP/EPR	DEN-T	RT	2.54	20-48	5-10	Effects of hygrothermal aging in different fluids	[96]
PP/EPR (15 wt%)	SEN-T	RT	2.5	13-57	12-35	Effects of orientation	[42]
PP/EPR (15, 21, 30 vol%)	DEN-T	RT	$6\text{-}1.8\cdot10^5$	15-30	3-8	Energy partitioning; effect of deformation rate (covering dynamic range)	[47]
PP/EPR (50/50 wt%)	DEN-T	RT	2	3-40	-	Strong dependence of the ethylene content of EPR; w_e via COD estimated	[140]
PP/EPR (10, 31 wt%)	DEN-T	RT	2	30-50	4-15	Effects of injection molding induced skin-core structure and orientation	[28]
PP/EPR and/or EBR/talc (60/30/10 wt%)	DEN-T	RT	50	9-19	-	w_e improvement with both EBR content and its molecular weight	[141]
PP/EBR (20 vol%)	DEN-T	RT	1	25-40	9-10	Morphology dependence	[64]
PP/EBR (5, 10, 15, 20 vol%)	DEN-T	RT	1	12-40	9-12	Dependence of blend miscibility via rubber composition	[142]
PP/POE (10, 25 wt%)	DEN-T	RT	10	3-23	3-17	Effects of draw ratio and draw direction (orientation)	[46]
PP/impact modifier (≤30 wt%)	SEN-T	RT	25	36-40	9-18	Comparison with J-integral – good agreement	[143]
HIPS/PE/SEBS (90/10/0-5 parts	DEN-T	RT	1	2-8	~0.5	SEBS compatibilizer enhanced w_e; energy partitioning	[144]

PS/SBS block copolymers (0-80/20-100 wt%)	DEN-T	RT	1	4-18	1-9	βw_p found to morphology sensitive parameter	[145]
Plasticized PVC/EVA (<9 phr)	DEN-T	23	5	13-20	5-6	Energy partitioning	[146]
PVC/CPE (<6 phr)	DEN-T	RT	10	8-15	-	Plane strain w_e determined; comparison with J-integral and G_c	[147]
PA66/rubber (7, 16, 25 wt%)	DEN-T	RT	1-500	27-42	7-12	Energy partitioning; effects of humidity and deformation rate	[81]
PA6/PP/SEBS-g-MA (54-90/0-36/0-10 wt%)	DEN-T	RT	2	5-35	-	Effect of orientation (injection molding); w_p computed	[148]
PA6/EBA (EBA-g-MA (binary and ternary blends)	DEN-T	RT	1	16-135	2-5	Compositional dependence	[149]
PA6/SB block copolymer also with MA grafting (≤30 wt%)	DEN-T	RT	10	153-180	27-44	Energy partitioning	[150]
RTPA66/LCP (80/20 wt%)	SEN-B	RT	5	4	~3	Good agreement between w_e and J-integral	[151]
PET/SEBS-g-MA (≤30 wt%)	DEN-T	RT	1	10-17	10-12	Data from quasistatic and impact tests collated	[152]
PET/EPR-g-GMA (≤20 wt%)	DEN-T	RT	1	7-26	0.5-12	Effect of aging	[153]
PET/rubber (core/shell particles) (7, 21 wt%)	SEN-B	RT	5	6-14	0-6	Effects of PET crystallinity and rubber functionalization	[154]
PET/PC (0-30 wt%)	DEN-T	RT	2-50	31-51	10-13	Effect of orientation; energy partitioning; both w_e and βw_p decreased with increasing PC content	[155]
PET/PPT	DEN-T	RT	1	27-40	8-11	Effect of compositional dependence	[156]

PBT/PPT (10-90/90-10 wt%)				30-65	8-12		
PBT/PC (commercial blend)	SEN-T, DEN-T	RT	2-50	30-38	3-5	Effects of specimen type and dimension	[157]
PBT/PC/modifier (commercial blend)	SEN-B	-196-50	5	5-14	-	Correlation with J-integral; effect of temperature	[158]
PBT/PC/modifier PC/ABS (commercial blends)	SEN-B, DEN-T, CT	25-70	5	9-11 11-14	-	Effect of specimen type; correlation with J-integral	[36]
PC/SB with and without MA grafting (star-shaped) (≤30 wt%)	DEN-T	RT	15	20-23	18-23	Rubber maleation improved w_e without affecting βw_p; energy partitioning	[159]

Table 7 EWF results on polymer micro- and macrocomposites under static loading

Matrix material	Additive	Specimen type	Testing conditions		EWF parameters		Comments	Literature
			T [°C]	v [mm/min]	w_e [kJ/m^2]	βw_p [MJ/m^3]		
LLDPE	GB (≤40 wt%)	DEN-T	25	5	18-58	7-12	w_e decreased with GB content; βw_p went through a maximum as a function of GB content; effect of GB size; reduced with filler content; w_e computed via COD	[160,161]
HDPE	Kaolin (≤30 vol%)	DEN-T	RT	0.2-2	1-24	2-6	Comparison with J-integral; direction dependence; w_e increased and βw_p reduced with filler content	[162,163]
HDPE/PET (85/15 wt%)	PET in microfibrils (MFC)	DEN-T	RT	5	7-37	<25	Effect of hot stretch ratio set to produce PET microfibrils	[164]
HDPE/PET (≤35 wt%)	PET in microfibrils (MFC)	DEN-T	RT	5	5-37	<25	Effect of composition at constant hot stretch ratio; w_p calculated via the shape factor (β)	[165]

HDPE/PET/EVA (85/15/≤2.5 wt%)	PET in microfibrils (MFC)	DEN-T	RT	5	38-56	18-32	Compatibilizer and transesterification catalyst improve both w_e and βw_p	[166]
PP	$BaSO_4$ (24 wt%)	DEN-T	RT	5	12-37	6-9	Effects of various coupling agents (best results with PP-g-MA and stearic acid)	[167]
PP-BC/PP-g-MA (≤7 phr)	$CaCO_3$ (1.8 μm) (≤30 wt%)	DEN-T	23	5	17-21	7-12	Energy partitioning; w_e slightly but βw_p was markedly reduced by increasing $CaCO_3$	[168,169]
PP /SEBS PP/SEBS-g-MA (≤20 wt%)	GB (10 vol%)	DEN-T	RT	1	15-29	1-7	w_p is strongly influenced by GB and rubber, whereas w_e is less affected	[170]
PP /PP-g-MA PP /SEBS PP/SEBS-g-MA (≤20 wt%)	SGF (23 wt%)	DEN-T	RT	1	8-32	2-20	Strong bonding between SGF and PP is detrimental to both w_e and βw_p	[171]
PP /SEBS PP/SEBS-g-MA (≤20 wt%)	SGF (30 wt%)	DEN-T	RT	1	12-48	1-23	Strong bonding between SGF and PP is detrimental to both w_e and βw_p	[172,173]
PP (≤20 wt%)	LGF (≤11 wt%)	DEN-T	RT	1	8-27	<2	Effects of thickness and orientation; w_e decreased with LGF content	[174]
PP /PP-g-MA (≤7 phr)	coal gangue powder (≤30 wt%)	DEN-T	23	5	15-22	6-12	w_e is less affected; βw_p strongly reduced as a function of coal powder; PP-g-MA as compatibilizer less efficient	[175]
PP-BC/ENR (≤9 phr)	coal gangue powder (20 wt%)	DEN-T	23	5	13-26	6-12	Energy partitioning; high ENR content enhanced w_e; βw_p was less affected	[176]
PP-BC/EPDM (≤30 phr)	coal gangue powder (≤100 phr)	DEN-T	RT	5	15-35	7-13	Both w_e and βw_p decreased with increasing filler content; correlation between w_e and notched Izod impact strength	[177]
PP/NR/LNR/PP-g-MA (70/20/10 wt%)	kenaf fiber (15 vol%)	DEN-T	RT	2	1.5-16	0.2-6	Kenaf untreated and treated with PP-g-MA strongly reduced both w_e and βw_p; failure followed by AE	[178]

PP PP/PET (95/5 wt%)	GB treated (50 wt%)	DEN-T	RT	2	8-12	0.6-3	Effects of specimen thickness and GB sizing; PET reduced both w_e and w_p	[179]
EPDM	GB treated (50 wt%)	DEN-T	RT	10	14-16	0.2-0.3	High adhesion (via silane) between EPDM and GB improved w_p	[180]
PA66/PP (75/25) PA66/PP/SEBS PA66/PP/SEBS-g-MA	SGF (20 wt%)	SEN-B	RT	5	4-10	0.5-1	Effect of MA grafting, comparison with J-integral (various determinations)	[181]
PA66/SEBS-g-MA (80/20 wt%)	SGF (≤35 wt%)	DEN-T	RT	1	7-32	2-14	w_e of the blend increased in the SGF range 5 to 20 wt%; βw_p monotonously reduced with SGF content	[182]
PA66/SEBS/SEBS-g-MA (80/20 wt%)	SGF (≤30 wt%)	SEN-B, DEN-T	20	5	12-26	0.3-12	maximum w_e at 10 wt% SGF; βw_p strongly reduced with SGF content	[183]
RTPA66	SGF (≤40 wt%)	SEN-B	RT	5	7-20	<1	Effect of processing; toughening mechanism discussed	[184,185]
RTPA66/EPDM (20 vol%)	SGF (≤40 wt%)	SEN-B	RT	5	7-12	0.1-16	maximum w_e at 10 wt% SGF; βw_p monotonously decreased with SGF content; toughening mechanism analysed	[151]
RTPA66/LCP (80/20 wt%)	SGF (≤20 wt%)	SEN-B	RT	5	<3	<1	Hybridization concept; good agreement between w_e and J-integral	[186]
PPC	Starch (≤30 wt%)	DEN-T	15	1	6-13	2-4	Starch incorporation reduced w_e and increased βw_p	[187]
PU	UHMWPE powder + short fiber (10 vol%)	DEN-T	RT	25	15-54	2-4	Effect of surface treatment of UHMWPE, w_e enhanced with increasing aspect ratio and surface treatment of the filler	[188]
PCL	Hydroxyapatite	DEN-T	not reported	not reported	32-64	6-16	Effects of specimen thickness and filler content	[189]

Table 8 EWF results on nanostructured, nanoreinforced systems under static loading

Matrix material	Additive	Specimen	Testing conditions		EWF parameters		Comments	Literature

		type	T [°C]	v [mm/min]	w_e [kJ/m^2]	βw_p [MJ/m^3]		
PE/PE-g-MA, compatibilizer (20 wt%)	OMMT (5 wt%)	DEN-T	RT	9	5-55	0.3-12	Effects of morphology and orientation; βw_p is sensitive for clay dispersion	[190]
LDPE/PE-g-MA (≤30 wt%)	LDH (≤15 wt%)	DEN-T	RT	1	2-25	0.2-5	Both w_e and βw_p reduced by increasing LDH content	[191]
HDPE/SEBS-g-MA (≤10 wt%)	OMMT (≤4 wt%)	DEN-T	70	1	6-29	2-7	SEBS improved both w_e and βw_p of the HDPE/OMMT nanocomposite	[192]
EVOH	OMMT (≤2.5 wt%)	DEN-T	23	10	30-90	3-12	Effect of orientation; w_p decreased with OMMT content	[193]
PP	MWCNT (≤5 wt%)	DEN-T	RT	1	<6	0.5-4.5	No self-similarity for load-displacement curves; CTOD rate estimated	[194,195]
sPP	OMMT (≤1 wt%)	DEN-T	RT	2	24-51	2-10	w_e increased but βw_p reduced by OMMT incorporation	[196]
PP/PP-g-MA (95/5 wt %)	OMMT (5 wt%)	DEN-T	RT	1-20	14-23	6-14	Energy partitioning; OMMT improved both w_e and βw_p	[197]
PP/PP-g-MA (4 wt %)	OMMT (2 wt%)	DEN-T	RT	1	4-16	0.3-2	Effects of manufacturing conditions; no self-similarities in the load-displacement responses	[198]
PP/PP-g-MA (2wt %)	OMMT (2 wt%)	DEN-T	RT	1	2-9	<0.7	OMMT dispersion; effect of the molecular weight of PP-g-MA; initiation values considered (energy partitioning)	[199]
PP/PP-g-MA/POE (≤6/≤20 wt %)	OMMT (<9 wt%)	DEN-T	RT	5	9-28	0.5-3	OMMT reduced both w_e and βw_p	[200]
PP/SEBS-g-MA (30/70 wt %)	OMMT (≤1.5 wt%)	DEN-T	RT	1	18-88	15-20	OMMT was efficient “toughener”	[201]
PP/SEBS-g-MA (≤20 wt %)	OMMT (≤4 wt%)	DEN-T	RT	10	18-26	5-25	OMMT reduced both w_e and βw_p	[202]
PP/NR/liquid NR	OMMT	DEN-T	RT	2	2-10	1-3	Both w_e and βw_p reduced by adding	[203]

(70/20/10 wt %)	(<6 wt%)						OMMT	
SBS block copolymers ABS/PS (≤80 wt %)	nanostructured per se	DEN-T	RT	1	<20	<8	Morphology dependence; strain field analysis; CTOD rate determined	[204,205]
PVC/ABS (100/20 wt %)	$CaCO_3$ (nanosized) (≤15 phr)	SEN-B	RT	2-10	8-18	3.5-5	w_e went through a maximum as a function of nano $CaCO_3$ content, while βw_p mostly decreased with filling	[206]
PA6	OMMT (0-3.7 wt%)	DEN-T	RT	1	200-400?	-	Effects of quenching; w_e decreased with increasing OMMT content	[207]
PA66	TiO_2 (21 nm) (≤3 vol%)	DEN-T	RT	1	7-19	0.3-1.8	w_e increased but βw_p decreased – only initiation values considered (energy partitioning)	[208]
PA66	TiO_2 (21 nm) SiO_2 (13 nm) Al_2O_3 (13 nm) (≤1 vol%)	DEN-T	23-120	1	5-22	<4	initiation values considered (energy partitioning); w_e via COD computed; both w_e and βw_p went through a maximum as a function of temperature	[209]
RTPA/rubber (≤10 wt%)	OMMT (<6 wt%)	DEN-T	RT	2	15-33	6-13	w_e reduced by increasing OMMT; w_p reduced by both rubber and OMMT content; effect of humidity; energy partitioning	[210]
PET	CB (25 nm) MWCNT (≤5 wt%)	DEN-T	RT	2	15-46	6-12	w_e reduced and βw_p went through a maximum as a function of nanofiller content; crazing studied by SAXS	[211]
BOPET/PS	PS nanolayered by printing	DEN-T	RT	2	46-66	1.3-2.5	Effect of nanolayered structure	[196]
PET	Aluminium layer (≤80 nm) by vapour deposition	DEN-T	RT	50	20-32	6-8	Effects of crystallinity and surface treatment of PET; effect of Al thickness; we decreased with PET crystallinity and increased with Al layer thickness	[212]
PC	MWCNT (≤6 wt%)	DEN-T	RT	1	<11	<3	Strain field analysis; CTOD rate determined; no self-similarities in the load-displacement responses (initiation	[213,214]

							should has been considered)	
PI	SiO_2 (≤5 wt%)	DEN-T	RT	0.2	34-38	0.6-0.9	FE calculation on the plastic zone; βw_p decreased monotonously with silica content	[215]
PI	SiO_2 (< 500 nm) (≤15 wt%)	DEN-T	RT-250	2	20-36	1.2-2.8	Both w_e and βw_p increased with the temperature	[216,217]

This is the right place to mention that the EWF was successfully adapted also for the qualification of welded joints of polymer/polymer systems. The related method is often termed essential work of interfacial fracture (EWIF) [218-220]

The tables above are not merely to inform the reader about the EWF tested materials, their testing conditions and major findings. The related results allow us to make some useful further comments. Considering for example the EWF data, achieved on the same polymer under comparable conditions by different groups, one can get an impression on "EWF-suitable" materials. Simply, the smaller is the scatter in the EWF parameters listed (i.e. w_e and βw_p) the more suited the corresponding material for EWF testing is. This aspect may be considered in the work ahead in respect to the standardization. Physical aging (below the T_g) and annealing (above the T_g but below the melting range) generally increase w_e at cost of βw_p. The same effect can be expected due to increasing crystallinity, incorporation of fillers and reinforcements. Note that the reinforcing effect of some additives may so strongly reduce the ductility of the material that the application criteria of the EWF do not hold anymore. For example, in many works done on nanocomposites the basic EWF criteria have been violated. Based on the works in which the testing temperature and deformation rate (strain rate, frequency) were varied, the following conclusions can be drawn:

i) w_e usually increases with increasing deformation rate and decreases with increasing temperature. For βw_p the opposite tendency holds.

ii) In the T_g range, and above, the material's ductility is enhanced. This yields a maximum in the βw_p term.

As far as other external parameters concern: water uptake (and similar effect owing to plasticising, felexibilizing) is accompanied with decreasing w_e and increasing βw_p. The combined action of water and temperature (hygrothermal aging) is material dependent: w_e may increase or decrease, however, βw_p usually decreases with aging time.

Comments on "orientation effect" in the tables are related to specimens which were cut in different directions from products produced by techniques resulting in processing-induced anisotropy in both amorphous and semicrystalline polymers. Molecular orientation (amorphous systems) and supermolecular structuring (semicrystalline systems) in the loading direction are connected with increasing w_e and decreasing βw_p when not blurring the EWF applicability itself. The above mentioned "supermolecular structuring" covers different morphologies like skin-shear-core layering, shish-kebab formation, work hardening due to polymorphic phase transition or spherulitic-fibrillar transitions etc., the detailed description of which is beyond the scope of this review. It is noteworthy that such structures are usually generated by injection molding, extrusion (blow) molding, uniaxial and biaxial hot stretching. Unfortunately, the (super)molecular parameters of the tested materials were scarcely reported and thus they can hardly be correlated with EWF parameters (see later).

3.2. Dynamic (impact) loading

The EWF method was extended to impact test using SEN-B specimens by Wu et al. [158]. The cited authors demonstrated that for elastic fracture w_e was equivalent to the critical energy release rate determined according to the linear elastic fracture mechanics. This initiated some debate whether or not the EWF is suited to assess the toughness under impact (dynamic) conditions. Based on the fact that the w_f vs. L curves on some polymers resulted in a negative slope and considering results from tensile tests, Vu-Khanh [24,221] concluded that the EWF is not appropriate for the impact fracture characterization of polymers. Negative slope, i.e. βw_p, was found also by other researchers [222]. However, in such cases the EWF preconditions were always violated. The usual problems are that a) though the fracture starts in a ductile manner but it turns to brittle in the remaining ligament; b) the ligament is not fully broken during the test (plastic hinge effect). González et al. proposed to consider only the fractured part of the ligament (true ligament) during the data reduction [223].

Vu-Khanh assumed that the fracture energy of a ductile polymer varies linearly with the crack extension and developed a model, that was [224,225] adopted by other researchers, too (e.g. [226]. Mai criticised this model [6,227] that the basic assumption does not hold and the model of Vu-Khanh is conceptually equivalent with that of the EWF.

The group of Paul [228-233] followed a phenomenological approach (i.e. not checking validity of EWF prerequisites) and introduced a different terminology (Equation (7)):

$$w_f = (u_0 + u_d \cdot L) \tag{7}$$

where u_0 is limiting specific fracture energy and u_d dissipative energy density. This was needed as the specimens were not conforming to the yielding criterion of the EWF. The first hint that the EWF conditions are not violated delivers the inspection of the specimens from their side: the stress whitened zone should be fully developed along the ligament. Recently, another proposal was made to come closer to the ligament yielding criterion: static preyielding of the specimens prior to their impact loading [223]. This is, however, highly problematic as the static loading-induced yielding is associated with structural rearrangements which manifests in an apparent crack tip blunting. It should be emphasized again that no such measures are needed if the EWF is adapted for 'suitable' polymers (i.e. fulfilling the above criterion) under dynamic loading.

Karger-Kocsis and Ferrer-Balas [234] have shown that amorphous copolyester fail ductilely even under tensile impact conditions. Since in the related DEN-T specimens no plastic zone formed, the cited authors used this finding to estimate the plane strain w_e value.

The Table 9 (polymers and polymer blends) and 10 (polymer composites) survey those works which were devoted to dynamic EWF measurements.

Table 9 EWF results on polymers and polymer blends under dynamic loading

Material	Specimen type	Testing conditions		EWF parameters		Comments	Literature
		T [ºC]	v [m/s]	w_e [kJ/m^2]	βw_p [MJ/m^3]		
LLDPE	DEN-T	RT	1	20-60	-	Effects of PE composition, orientation and processing morphology	[235]
UHMWPE	DEN-T	RT	3.7	16	21	Compared to quasistatic tests w_e reduced but βw_p increased	[236]
PP-RC	SEN-B	RT	1.8	8.3	~3.7	Correlation with static J-integral	[237]
PP-RC, PP-BC	DEN-T, SEN-B	RT	1.8	8	<4	Statistical analysis of the EWF testing; effects of specimen thickness and specimen type	[238,239]
RTPP (26 vol% rubber)	SEN-B	RT	1.8	5.7	-	Good agreement with dynamic J-integral	[240]
ABS	SEN-B	RT	3.7	16-17	0.1-0.8	Referred as plane strain value	[236]
ABS	SEN-B	-25-25	3.5	~2	5-8	βw_p decreased with decreasing temperature; w_e invariant with temperature	[232]
ABS	SEN-B	22	1.06	~3	2.1	-	[241]
ABS	DEN-T, SEN-B	RT	3.5	12	<0.5	Statistical analysis of the EWF testing; effects of specimen thickness and type	[238,239]
ABS (25 vol% rubber)	SEN-B	RT	1.8	1.9	-	Good agreement with dynamic J-integral	[240]
PET (semicrystalline)	DEN-T	0-70	1	60	18	Both w_e and βw_p increased with increasing deformation rate (from static to dynamic); energy partitioning; master curve generated	[242]
PCTG	DEN-T	RT	1.2	17	5	Plane strain value as yielding-related w_e defined	[234]
PP+PP-g-MA/SEBS+SEBS-g-MA (80/20 wt%)	SEN-B	21	3	1.5-8	<0.2	Rubber incorporation enhanced w_e	[243]
PA6/POE-g-MA amorphous PA/POE-g-MA	SEN-B	RT -25-25	3.5	1-8	0-9	Dependence of the morphology; also linear elastic fracture mechanics; strongly influence of rubber particle size on both w_e	[228]

(<20 wt%)						and βw_p	
PA6/different rubbers (EPR, EPR-g-MA, SEBS, SEBS-g-MA) (80/20 wt%)	SEN-B	RT	3.5	17-32	0-11	Dependence of the morphology; also linear elastic fracture mechanics	[231]
PA6/PPE/SMA+SEBS (50/50/5 wt%; <20 phr)	SEN-B	20-100	3	18-26	1.3-2.5	Morphology assessed, toughness mechanism deduced	[244]
PA6/ABS (rubber: 45 wt%)/acrylic (55/40/5 wt%) (70/25/5 wt%)	SEN-B	-25-25	3.5	4-7 3-4.6	9-17 11-13	βw_p decreased with decreasing temperature; w_e invariant with temperature	[232]
PA6/ABS (compatibilizer (various)	SEN-B	25	3.5	1.5-25	0.1-2.6	Morphology and compositional dependence; correlation with notched Charpy	[245]
PA6/EPR-g-MA (≤20 wt%)	SEN-B	RT	3.5	2-11	0-4.5	Both w_e and βw_p increased with rubber content	[229]
RTPA6 (rubber: 10 and 25 wt%)	SEN-B cantilever (IZOD)	23	2	12-20	-	Effects of testing configuration and notch type; ductile/brittle transition	[246]
PBT/PC (impact modifier)	SEN-B	-196-100	2.96	<13	-	Correction for kinetic energy; w_e passes a maximum as a function of temperature	[158]
PBT/POE-g-MA (≤30 wt%)	SEN-B (IZOD)	RT	~3	0-30	0-8	Notched impact strength and βw_p have identical compositional dependences; brittle/ductile transition traced to morphological changes	[247]
PC/ABS (100/0; 60/40)	SEN-B	22	1.06	1-7	<2.4	Effect of strain rate; different fracture mechanical approaches	[241]

Table 10 EWF results on polymer composites under dynamic loading

Matrix material	**Additive**	**Specimen type**	**Testing conditions**		**EWF parameters**		**Comments**	**Literature**
			T [°C]	**v [mm/min]**	**w_e [kJ/m^2]**	**βw_p [MJ/m^3]**		

HDPE/SEBS-g-MA, (≤10 wt%)	OMMT (≤4 wt%)	SEN-B	19	1.8	4-12	0.1-2	With increasing OMMT both w_e and βw_p reduced	[192]
Poly(ethylene-co-methacrylic acid) ionomer	OMMT (≤10 wt%)	SEN-B	RT	3.4	2-20	<0.9	w_e showed a maximum at 2 wt% OMMT; βw_p decreased monotonously in function of OMMT content	[233]
PP-H/PP-BC (≤29 vol%)	SGF (15 vol%)	SEN-B	20	2	<4	~0	Correlation with notched Charpy results; effect of impact modifier on the w_e of the composite is very small	[248]
PP/SEBS-g-MA (≤20 wt%)	OMMT (≤4 wt%)	SEN-B	RT	1.8	1.3-9.5	<0.4	SEBS-g-MA improves both w_e and βw_p, whereas OMMT has an adverse trend	[249]
RTPP (rubber: SEBS, SEBS-g-MA (15 wt%)	SGF (23 wt%)	SEN-B	21	0.5-5	3-8	<1.1	Dependence of impact rate; effect of maleation	[250]
RTPP (rubber: SEBS, SEBS-g-MA (≤20 wt%)	SGF (23 wt%)	SEN-B	21	3	6-12	-	βw_p was absent for the SGF reinforced versions; rubber toughening increased w_e	[243]
PA6/EPR-g-MA (≤20 wt%)	SGF (≤20 wt%)	SEN-B	RT	3.5	<25	0-4.5	w_e increased with increasing rubber or SGF content ; βw_p increased with increasing rubber or decreasing SGF content	[229]
PA6/SEBS-g-MA (≤20 wt%)	OMMT (4 wt%)	SEN-B	21	3.4	<20	<2.5	with increasing SEBS-g-MA both w_e and βw_p increase; OMMT incorporation results in adverse tendencyreduced by SGF content	[251]
PA66/SEBS-g-MA (80/20 wt%)	SGF (≤30 wt%)	SEN-B	21	3	12-26	~0	w_e is reduced by SGF content; no βw_p registered as SGF restricted the shear yielding of the matrix	[252]
PA66/SEBS+SEBS-g-MA (80/20 wt%)	SGF (≤30 wt%)	SEN-B	20	3	8-22	0.1-9	minimum of w_e at 10 wt% SGF; both w_e and βw_p reduced by SGF content	[183]
PA1010/POE-g-MA (0; 20 wt%)	SGF (≤25 wt%)	SEN-B	RT	3.5	16-21	1-12	maximum w_e at 10 wt% SGF; βw_p monotonously decreased with the SGF content	[253]

Based on the dynamic (impact) EWF results no general conclusions can be deduced. This is due to the fact that the validity criteria were not checked and the testing conditions (deformation rate, temperature) not varied in most of the published works. From the viewpoint of testing, it is recommended to keep 1 m/s as deformation rate to avoid oscillation phenomena at higher speeds. External cushioning of the specimen (Charpy- and Izod-configurations are preferentially used) or striker is not necessary because of the high damping of EWF-suited polymer systems. Further works are needed, however, to summarize effects of material-related internal (morphology, plastification, aging etc.) and testing-related external parameters (temperature, deformation rate) on the EWF characteristics.

4. EWF UNDER MODE II LOADING

The applicability of EWF mode II (in plane shear) loading was checked by Kwon and Jar [254,255]. The cited authors used a Iosipescu test set-up to apply the shear force on a specimen with edge notches. Between the notch tips V-shaped grooves were introduced along the specimen surface, i.e. parallel to the shear loading direction. The failure mode during loading has been surveyed. This is proved to be useful to differentiate between mode II and mode I type loadings. The latter occurred in the final stage of fracture through fibrillation. In case of ABS it was found that the specific work of fracture (corrected for the work needed for the cracking of the shear plane) is independent of the ligament of the specimen (DEN-Shear), but depends on the groove thickness. This relationship was used to determine the shear essential work of fracture that was found more than two times higher than under mode I loading at the same deformation rate (2.5 mm/min) [254]. In a companion work HDPE was the sample material. Unlike to ABS, the corrected specific work of fracture of HDPE depended also on the ligament length. The authors proposed another data reduction method which eliminates the energy consumption due to ligament rotation and plastic deformation for this polymer. Similar to ABS w_e under mode II proved to be ca. twofold of w_e in mode I also for HDPE [255].

It is interesting to note that EWF has not been adapted to PETG, PCTG materials under mode II, though they are considered as best model materials for the EWF [12,103]. Moreover, being birefringent, the stress development in these amorphous copolyesters could be followed by stress optical measurements. Apart of the Iosipescu test set-up other methods may also be of interest. For example the ball shear test might be adapted to study the properties of weld seams of polymers [256].

It is the right place to underline that polymers usually do not fail under pure (in plane) shear in microscopic level. This is not even the case for unidirectional composite laminates in which the matrix is under constraint favouring pure mode II deformation. The appearance of patterns with hackles (brittle thermosets) and torn fibrils (ductile thermoplastics) in such composites evidences the non-localized shear failure.

5. EWF UNDER MODE III LOADING

Tear resistance of thin materials can be determined using trousers specimens, and the related method was developed by Rivlin and Thomas for the investigation of rubber [257]. This type of specimen was used first by Mai and Cotterell [7] for the toughness assessment of a ductile metal by adopting the EWF theory. To determine the specific tearing essential work of fracture parameter (w_{TE}) the cited authors derived a schema which takes into account the work needed for bending and unbending of the specimen [7]. However this work on ductile polymer films is negligible because of their low stiffness, so this approach cannot be used directly for polymer films. Wong et al. have published a two-zone model for polymeric material [258]. According to this concept, the tearing fracture process in ductile polymers can be divided into two parts. The initial zone, where the crack starts and the outer plastic zone (h) increases continuously with the torn ligament length (Zone A). At the end of Zone A the height of plastic zone (h_B) remains constant and during further crack propagation h_B does not change. This "saturation" region is called Zone B – cf. Figure 6a. Figure 7 shows that in this trousers tearing test a well developed plastic zone appears in the preferred amorphous copolyesters. In Zone A the following procedures take place:

1. The constant load results in the straightening of the legs, hence the shape of the crack tip changes continuously.
2. Significant changes occur in the fracture mode: in-plane (Mode I) becomes dominant against out-of-plane (Mode III), due to the turning of the crack tip region into plane of the load.
3. The height of the plastic zone (h) increases simultaneously with the crack propagation.

The total tearing work in Zone A is given by Equation (8) [258]:

$$\frac{W_{TF}}{L_a t} = w_{TF} = w_{TE} + \alpha'' w_{TP} L_a \qquad (8)$$

where L_a is the length of the torn ligament in Zone A ($0 < L_a \leq L_A$), L_A is the ligament length at the end of Zone A and α" is a shape factor which can be determined with Equation (9) in case of a semi-elliptical plastic zone:

$$\alpha'' = \frac{\pi h_B}{4 L_A} \qquad (9)$$

Note that the subscripts T, E and P signify the tearing fracture, and the related essential and non-essential (plastic) contributions. In the $0 < L_a \leq L_A$ region the specific tearing essential work (w_{TE}) can be obtained by reading the y intercept of $w_{TF} - L_a$ curve.

From the end of Zone A ($L_a = L_A$) in Zone B the height of the plastic zone remains constant (h_B=const.) during further crack propagation. In Zone B the total specific tearing work (w_{TF}^{B}) can be written Equation (10) based on the EWF method [258]:

$$w_{TF}^{B} = \frac{W_{TF}^{B}}{L_B t} = w_{TE}^{B} + w_{TP}^{B} h_B \qquad (10)$$

where L_B is the ligament length in Zone B.

If trousers with different plastic zone heights are prepared w_{TE}^{B} can be determined (according to Equation (10)) from the y intercept of w_{TF}^{B} -h_B plot. Nevertheless, for many polymers the change in h_B is too small and thus the related change can hardly be detected. Therefore w_{TE}^{B} is usually defined by Equation (11) [258,259]:

$$w_{TF}^{B} = \frac{2F_s}{t} \qquad (11)$$

where F_s is the saturation tearing force in Zone B.

h_B can be measured on the torn trousers specimens directly, and w_{TP}^{B} is equal to the slope of the regression line in Zone A ($w_{TP}^{B} = w_{TP}$) thus w_{TE}^{B} can be determined according to Equation (10). Wong et al. has published similar values for EWF parameters in Zone A and B for PETG and PP [258].

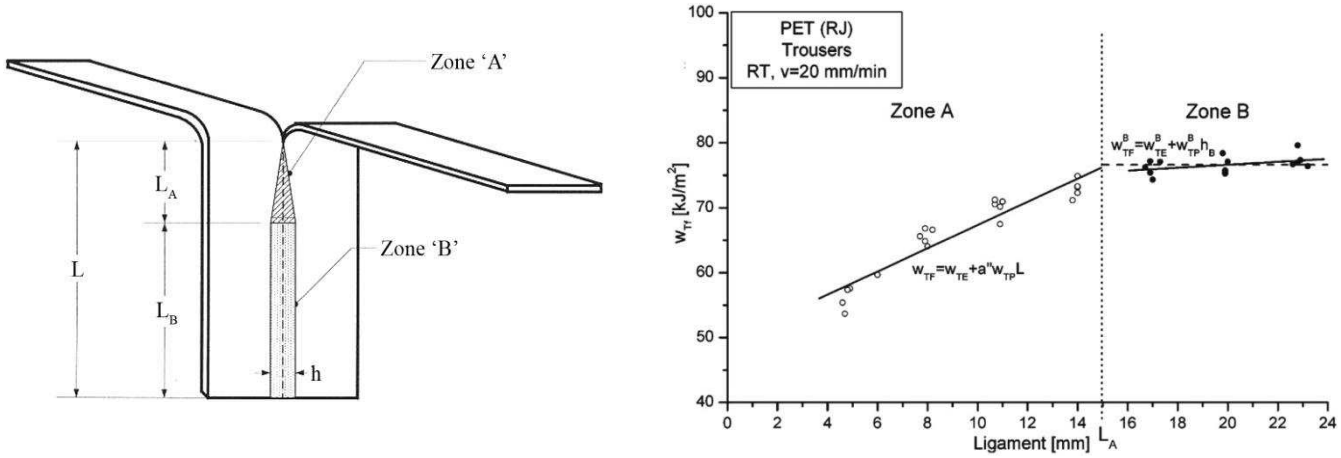

(a) (b)

Figure 6 Schematic diagram showing the fracture zones on the trousers specimen (a) and evaluation of out-of-plane EWF results (trousers) of PET (b) [94] (Picture b: reprinted from: Bárány T., Ronkay F., Karger-Kocsis J., Czigány T.: In-plane and out-of-plane fracture toughness of physically aged polyesters as assessed by the essential work of fracture (EWF) method. International Journal of Fracture, 135, 251-265 (2005), Copyright 2005, with permission from Springer Science + Business Media)

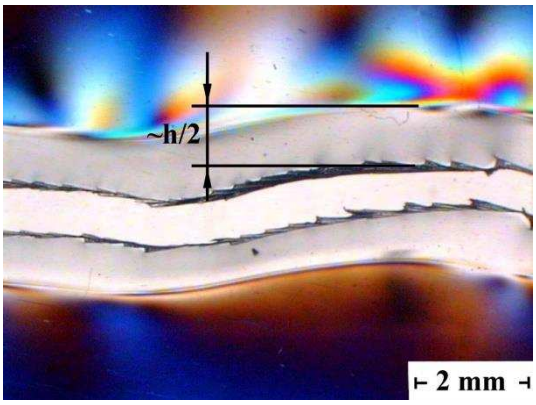

Figure 7 Cross polarized image of the plastic deformation along the tear path within zone B for an amorphous copolyester

6. CORRELATIONS

6.1. EWF parameters under different loading modes

Only few studied addressed the comparison of EWF parameters determined under different loading conditions. Majority of the conducted works focused on mode I and mode III [23], and only two [254,255] compared the mode I and mode II responses. It has to be underlined, that no work addressed so far the comparison of EWF parameters deduced from mode I, II and III type loadings.

Mode I and III

Trouser type tear tests were preferred to determine the mode III toughness of films. In many cases, however, it has not been checked whether the prerequisites of the EWF application are fulfilled. The yielding-related criterion was likely not met as the onset of plastic zone in the specimens was never mentioned. In the related studied (e.g. [89,121,259-261]) it was assumed that Equations (12) and (13) are valid:

$$w_f = \frac{2F}{t} \tag{12}$$

and

$$w_p = \frac{F}{t^2} \tag{13}$$

where F is the tearing force and t the thickness of the tested sheet, film.

The agreement between the mode I w_e measured on S(D)EN-T specimens and w_{TE} measured on trousers specimens and calculated by Equation (12) was poor, or in the best case fair. A similar note holds also for the corresponding w_p data. In addition, contradictory results are available on whether the mode I or III type EWF parameters are higher.

Follow-up works used amorphous copolyesters as model materials to collate mode I and III EWF results [94,258,262]. Wong et al. [258] has investigated two kind of PPs (homo- and block copolymer (EPBC))

and PETG films with different thicknesses and at different testing temperatures (in case of PETG). However, only for PETG having thickness of 0.2 mm and for EPBC was observed good agreement between the w_e and w_{TE} values. On the other hand, Bárány et al. [94] found a very good agreement between the w_e and w_{TE} values in case of thermally aged polyester (PET, PETG) films (cf. Figure 8).

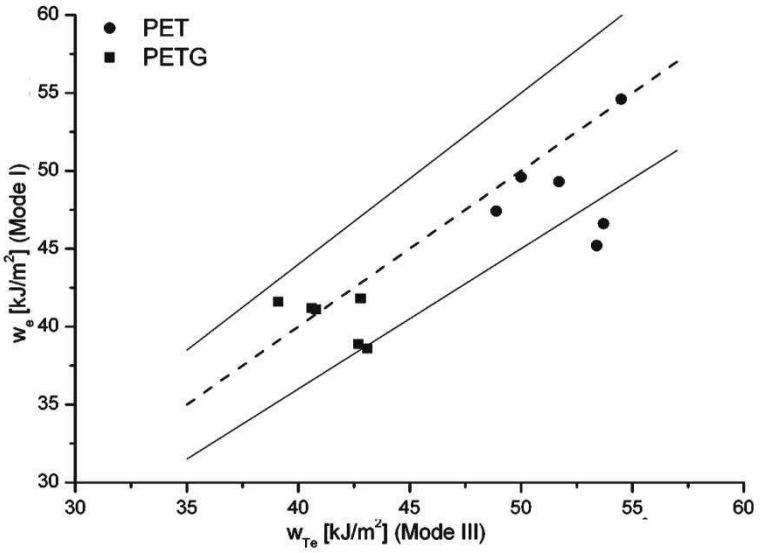

Figure 8 Correlation between in-plane and out-of-plane EWF results [94] (Reprinted from: Bárány T., Ronkay F., Karger-Kocsis J., Czigány T.: In-plane and out-of-plane fracture toughness of physically aged polyesters as assessed by the essential work of fracture (EWF) method. International Journal of Fracture, 135, 251-265 (2005), Copyright 2005, with permission from Springer Science + Business Media)

Fair agreement between mode I and III type w_e values has been reported also by Kim and Karger-Kocsis [262]. The cited authors, proposing a three-zone model, underlined that w_{TE} depends also on the thickness of the sheet. This was traced to differences in the development of the plastic zone. A similar conclusion was drawn by Yuan et al. [263] who modified the two-zone tearing fracture concept.

Mode II and III

As mentioned before Kwon and Jar have shown that mode II (shear mode) w_e is more than twofold of mode I w_e based on the results achieved on ABS [254] and HDPE [255], respectively. The authors of this paper are convinced that mode II tests have to be done on amorphous copolyesters in order to get a clearer picture on this issue.

6.2. EWF and other fracture mechanical parameters

For ductile polymers apart of the EWF the crack tip opening displacement (CTOD) and the J-integral are commonly used. All of them belong to the group of nonlinear fracture mechanics.

The CTOD criterion is linked to the crack opening prior to extension. CTOD thus also considers the plastic flow capability of the polymer. The basic problem with this method is that many polymers tend to craze or to flow instead of exhibiting homogenous plastic deformation. The latter is reflected by smooth

crack tip blunting. Anyway, the CTOD is a very straightforward technique when effects of the initial microstructure are considered.

Hashemi and O'Brien [120] proposed a way to estimate the w_e via crack opening displacement (COD) that was simplified later [85]. This approach entails plotting the extension of the specimen at failure (x_b) against the ligament (L). x_b is read from the F-x curves. Under plane-stress condition a linear relationship is anticipated in form of Equation (14):

$$x_b = x_0 + x_p \cdot L \tag{14}$$

where x_0= COD, and x_p is the plastic contribution of extension. w_e can be calculated by Equation (15):

$$w_e = \sigma_y \cdot x_0 \tag{15}$$

where σ_y is the yield strength of the corresponding polymer. Note that the above relationship is in close analogy with that introduced by Wells for the determination of G_c [264].

It was demonstrated that Equation (15) is well suited to estimate w_e and stress concentration effects (cf. Hill's criterion) should not be considered [102].

The possibilities to calculate w_e via the COD was explored in many papers. They are mentioned in the tables indicating "w_e via COD computed" or the like.

The EWF method is analogous to the J-integral, as both of them represent a type of the resistance (R) curves. There are also some similarities between the J-integral and EWF from the viewpoint of testing (multiple specimen technique) and data reduction (linear relation). So, the resistance to crack growth (J_R) is a linear function of the crack extension (Δa) (Equation (16)):

$$J_R = J_c + \frac{dJ}{da} \cdot \Delta a \tag{16}$$

where J_c is the critical or initiation value. The authors do not want to go deeper in this topic by considering other data reduction methods (via power law function, consideration of blunting etc.)

Mai and Cotterell [6] have shown that for DEN-T and DCN-T specimens Equation (17) holds:

$$w_f = J_c + \frac{L}{4} \cdot \frac{dJ}{da} \tag{17}$$

Accordingly $w_e = J_c$ and $\beta w_p = \frac{1}{4} \cdot \frac{dJ}{da}$. This has been confirmed in several papers as indicated in the tabulated results ("comparison with J-integral" and the like). Although good numerical agreement was usually found between w_e and J_c, it is questionable whether or not w_e represents an initiation value. The latter is the case, however, when considering the related energy partitioning methods disclosed in Figures 2a and 2b.

It is the right place to call the attention why the EWF became for more popular than the J-integral. The determination of the crack extension (Δa) for the J-integral is not an easy task. In addition, there is some uncertainty or how to define the blunting and thus derive J_c. All these problem are circumvented in case of the EWF due to the specimens (different ligaments) and data reduction (w_f intercept).

6.3. EWF and other (toughness) tests

EWF parameters were often correlated with those from other toughness tests even if they deformation rates (strain rate, frequency) differed markedly from that of the EWF test. So, static EWF vs. static tensile (work of fracture), static EWF vs. dynamic impact data (Charpy, Izod, falling weight), dynamic EWF vs. dynamic impact data (see the data in Tables 9 and 10) are already collated, and mostly a good correlation between them was reported. Attempts were also made to correlate EWF results with other properties which are not directly toughness-related ones. For example the life expectation of HDPE pipe materials was forecasted by considering EWF results [38]. For the modelling of the drop impact properties of fluid-filled PE containers the EWF results were considered as important input material parameters [265].

7. UNSOLVED ISSUES

7.1. Plane stress and plane strain data

Ductile-brittle transition in the fracture of the specimens often resulted in misinterpretation of the results, and even to discrediting of the EWF concept (due to negative slope of the w_f vs. L traces). To overcome this problem researchers kept more strictly the ligament criterion of the EWF specimens or attempted to consider only the ductilely failed part of the ligament [26,223]. To determine the plane strain specific essential work of fracture was triggered by the research policy that this value, representing the intrinsic toughness, should be related to the (super)molecular characteristics of the corresponding polymer.

Plane stress – plane strain transition (also referred to mixed mode stress state) occurs when the size of the ligament becomes comparable with the thickness of the specimen. This is accompanied with a strong plastic constraint in the notch tip. However, the mixed mode stress state will be purely plane strain at L=0 (Figure 9).

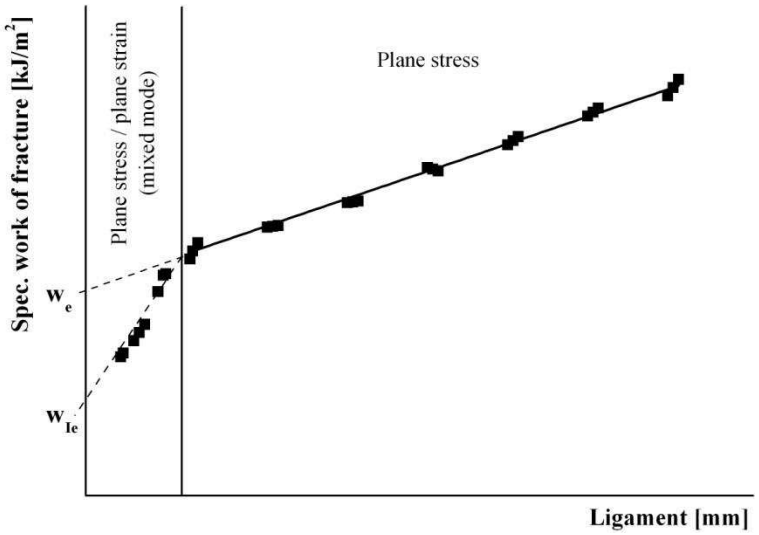

Figure 9 Effect of the ligament length on the stress state in DEN-T specimens schematically

Accordingly, Mai and Cotterell [6,9] recommended that the plane strain value (w_{Ie}) can be determined by linear extrapolation to L=0 of the w_f vs. L data in the mixed mode regime. This proposal was followed and compared with other fracture mechanical data by many researchers (they are mentioned in the tables under 'plane strain value'). Saleemi and Nairn [20] took into consideration that $w_e=f(L, t)$ and βw_p is invariant with L. They considered w_{Ie} as the extrapolated value of the (w_f - $\beta w_p L$) vs. L curve at L=0.

Karger-Kocsis and Ferrer-Balas [234] followed another concept. They suppressed the development of the plastic zone by high deformation rate tests (namely tensile impact) and made use of the energy partitioning method described first in ref. [12]. They argued that the yielding-related specific work of fracture ($w_{e,y}$), determined under static loading, agrees well with the concluded plane strain value from dynamic loading. This method has been questioned by Mai et al. [6] emphasizing that the followed data reduction disregarded possible effect of the specimen thickness.

A recent energy partitioning approach of Kwon and Jar [266] is basically similar to that of Karger-Kocsis [12]. The model material of the authors (HDPE) showed, however, no well detectable yielding, but a complex failure mode. Excluding effects of the severe plastic deformation and fracture of the surface layers of the specimen and plotting the related energy vs. L a thickness independent plane strain value was derived. This method is also questionable as the detection of the load threshold, accompanied with fracture in the mid section of the specimen is not well detectable, and in addition likely strongly dependent on the polymer itself. Moreover, the plane strain value is connected with post yield energy data according to the proposed energy partitioning. In a follow up work Ben Jar and Adianto [267] used the energy partitioning of Mai and Cotterell [9] keeping, however, the earlier model to deduce w_{Ie}.

The above discussion clearly demonstrates that the estimation, determination of the plane strain essential work of fracture (w_{Ie}) is still topic of intensive dispute. For its settling further investigations are needed using suitable, "EWF-conform" polymers.

7.2. Dependence on structural parameters

Accepting that the toughness is an inherent material property, it should rely on structural parameters of polymer systems. To elucidate the effects of microstructure (composite systems), morphology (semi-crystalline polymers) and molecular characteristics (semi-crystalline and amorphous polymers) on fracture mechanical data (determined by linear and nonlinear elastic fracture mechanics), the corresponding tests should be performed on series of samples in which the structural parameters varied are not interrelated. Albeit this requirement is obvious, it can hardly be fulfilled for semicrystalline polymers and related composites. Note that in such systems molecular, morphological and microstructural (due to fillers and reinforcement) are strongly interrelated. For instance, it is well known that changes in the molecular weight (MW) affect the crystallinity, the lamellar build-up and arrangement, the density of the tie molecules etc. – so which one should be considered as control parameter? The scenario becomes even more complex due to processing since it may blur the effects of the initial (super)molecular

structure. The latter is changing also during loading of the specimen. This rises the question: is there any way to trace effects of the initial structure on the toughness (i.e. EWF response in this case)?

Considering the R-curve of w_f vs. L, w_e (or more exactly its critical value under plane strain condition) should represent the resistance to crack initiation. On the other hand, the slope of the w_f vs. L curve, i.e. βw_p, is a direct measure of the resistance to crack propagation. It is intuitive that the resistance to crack initiation, i.e. w_e, depends on the initial structure. By contrast, the resistance to crack propagation, i.e. βw_p, is strongly affected by strain-induced structural rearrangements. The next question is: how to split the effects of the initial structure from that of the strain-induced one? Recall the often stressed but very often ignored prerequisite of the EWF: full ligament yielding prior to crack growth! This behaviour allows us to distinguish between effects of the initial and loading-modified microstructure. In terms of the EWF it means that energy-partitioning (for example splitting for yielding and necking+tearing as shown in Figure 2b) is the straightforward technique to conclude effects of the microstructure. Finding correlations between the molecular and EWF parameters is an easier task for amorphous than semicrystalline polymers as it well be demonstrated. However, a further restriction should be made: the amorphous polymer should fail by shear deformation instead of crazing. Note that crazing is associated with considerable work hardening and thus blurs the effect of the initial structure. For that purpose amorphous copolyesters are the right materials.

Karger-Kocsis and Moskala [103] studied the EWF response of such thermoplastic copolyesters as a function of their intrinsic viscosity (correlates with MW). It was demonstrated that the yielding-related essential work of fracture ($w_{e,y}$) did not depend on the MW. On the example of amorphous PEN it was shown that MW affects only the necking+tearing term [25]. So, if not MW, what else may control the EWF of amorphous polymers? It was early recognized that the molecular entanglement plays a decisive role in this respect. Karger-Kocsis et al. [25,99,103] have shown that the plastic zone of the DEN-T specimens of amorphous copolyesters diminishes after subjecting them to heat treatment just above their T_g (cf. Figure 10). This “healing”, shape-recovery is due to the onset of a stretched entanglement structure which is the driving force for also in the most simple shape memory polymers [268,269]. As the network stretching was not accompanied by voiding, crazing, or strain-induced crystallization, the related polymers were concluded as the most suited ones to study MW effects. However, it is noteworthy that the stretching (cold drawing) affected the cold crystallization of the material just above its glass transition temperature (T_g) as proved by modulated DSC [270,271].

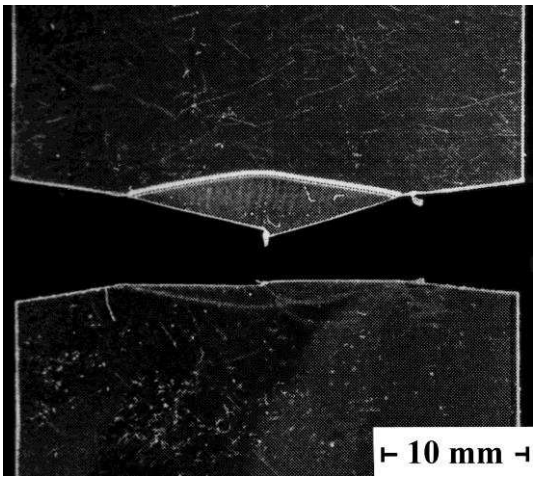

Figure 10 DEN-T specimen of an amorphous PEN before (upside) and after (downside) heat treatment [25]

(Reprinted from: Karger-Kocsis J., Moskala E. J.: Molecular dependence of the essential and non-essential work of fracture of amorphous films of poly(ethylene-2,6-naphthalate) (PEN). Polymer, **41**, 6301-6310 (2000), Copyright 2000, with permission from Elsevier)

As a consequence, it was proposed that the entanglement network and its characteristics control the inherent toughness of amorphous polymers. Later Karger-Kocsis succeeded to substantiate this claim by plotting $w_{e,y}$ as a function of the square root of the mean entanglement molecular weight (M_e) – cf. Figure 11 [272]. Note that this function, provided that linear, is analogous to that deduced for crosslinked rubbers. Recall that $w_{e,y}$ was considered by the cited author as plane strain value (as disclosed in section 7.1).

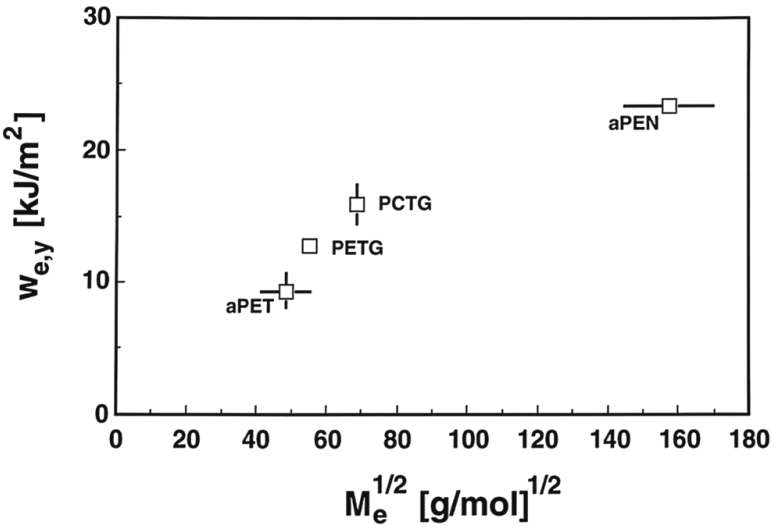

Figure 11 Yielding-related essential work of fracture vs. square root of the mean molecular weight between entanglements [272,273] (Reprinted from publication: Karger-Kocsis J.; Fracture and fatigue behavior of amorphous (co)polyesters as a function of molecular and network variables. in 'Handbook of Thermoplastic Polyesters' (ed.: Fakirov S.) Wiley-VCH, Weinheim, 717-753 (2002) Copyright Wiley-VCH Verlag GmbH & Co. KGaA. Reproduced with permission)

It was also supposed that the necking-related essential work of fracture ($w_{e,n}$) should linearly change with the entanglement network density. The related trend underlied, however, a large scatter. This suggested

that apart of the entanglement network density other parameters, like chain build-up, flexibility, may also be at work. An indirect proof for this assumption was delivered by Chen et al. [104] using amorphous copolyesters of various molecular build-up. A linear dependence of w_e on M_e, or in case of crosslinked system, M_c (mean molecular weight between crosslinks) has been proved by Chen and Wu [123]. The cited authors concluded that w_e is required to deform and break the chain segments of the physical (or chemical) network, across the ligament. Based on this concept the above authors developed a theoretical model to explain the molecular dependence of the EWF [122]. According to this model w_p is the energy needed for "fully plastic extending the network in the plastic zone".

Compared to amorphous polymers, the relationship between EWF toughness and molecular, morphological parameters of semicrystalline polymers is far less understood. In the literature highly contradictory data can be traced on how the toughness is affected by molecular and supermolecular variables. This can be reasoned by the fact that one single parameter of the crystalline structure can hardly be varied without affecting some others. Variation in the degree of crystallinity for example is associated with manifold changes both in the spherulitic structure (type, size) and within its constituents (thickness and order of lamellae, amorphous layer thickness tie molecules density). According to the model of Karger-Kocsis the toughness goes through a maximum as a function of the degree of crystallinity (cf. Figure 12) [11,273]. The increasing left hand flank of the curve represents the resistance resulting from the crystalline structure, while the declining one signifies that the toughness response is controlled by the "weaker" contribution. There are many indirect hints for the validity of the model depicted in Figure 12, however, an elegant experimental evidence is still lacking. One should also keep in mind that the tie molecules density is affected by the mean MW because its value increases with the MW. The authors' feeling is that the abovementioned strong interaction between the structural parameters in semicrystalline polymers necessitates a complex statistical evaluation. This is probably the right tool for "data mining" as demonstrated by Egan and Delatycki [274].

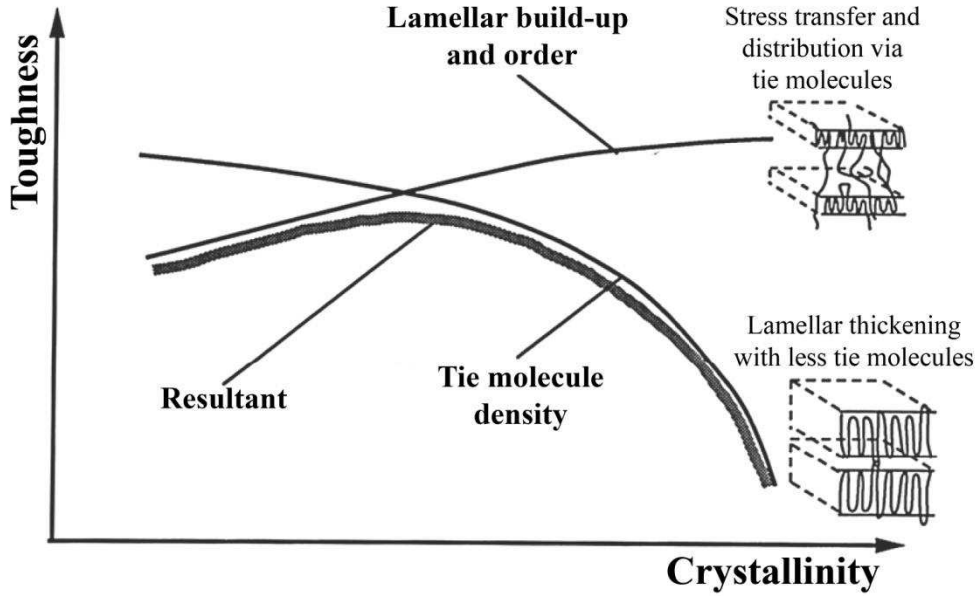

Figure 12 Predicted change of toughness as a function of of crystallinity (after Refs. [11,273])

Among the other internal parameters short chain branching was found to affects the crystallinity and morphology. This effect has already been studied on the example of LLDPEs by the EWF method [235]. The increased toughness by increasing short chain branch length is likely due to a similar change in the tie molecule density. Fayolle et al. [275] varied (reduced) the MW of PTFE by γ-irradiation and concluded that the mean MW should be about 50 times higher than the M_e in order to avoid a ductile-brittle transition during the EWF test. Sheng et al. [57] reported that w_e linearly changes with the number average MW and βw_p decreases with increasing Z average MW of PP-BC. Karger-Kocsis [64] concluded that w_e is enhanced by the order of the crystalline structure and by increasing tie molecule density (transferring the stress from the "weak" amorphous to the "strong" crystalline phase). βw_p, on the other hand, is controlled by the stress redistribution process in the plastic zone. This is strongly influenced by loading-induced possible changes in the local morphology. Accordingly, the crack growth behaviour depends on the mode and rate of the morphological and molecular rearrangements in the plastic zone. His major conclusion was that between w_e and βw_p an inverse correlation exists and thus the resistance to crack initiation and growth should be compromised for a given material.

Note that in this part of the review effects of the processing-induced structure have not mentioned yet. Such effects, covering higher order structure (skin-shear-core morphology), enrichment/depletion of fillers, orientation and layering of discontinuous fibrous reinforcements etc., have a strong impact on the EWF behaviour. Their overall effect may be so severe that the EWF prerequisites are no more fulfilled. A good example for that is the crack deviation due to the injection molding-induced skin-core structure [28]. This scenario is associated with high "ductility level" according to the terminology of Martinez et al. [23]. Effects of processing-induced microstructure have been usually considered in the related works, for example by cutting the specimens in machine and transverse direction. In the tables before the comments "effect of orientation" or similar notes indicate for the anisotropy in the corresponding materials, which is always well reflected in the EWF parameters.

8. CONCLUSION AND OUTLOOK

Albeit some works are still in progress on the testing methodology (notching [15-17,23,93], specimen selection, validity criteria, energy partitioning, data reduction [276], modelling [277-279] and even alternative w_e determination [280-282], the EWF method seems to be well established. Therefore we can assume that the existing ISO draft will be a standard soon. Users, however, have to learn that the EWF method cannot be adapted universally. The guide lines for its proper use are clearly outlined in this contribution.

Unsolved problems with the EWF are linked with its extension for plane strain condition, and even more gravely, with the molecular and microstructural dependence of the EWF parameters.

The toughness of amorphous polymers depends unambiguously on characteristics of the entanglement network structure. Further work is needed, however, to separate effects of the initial physical network (likely related to the toughness at fracture initiation) from that of the loading-induced one (fracture propagation resistance).

The microstructural dependence of fracture mechanical parameters is far less understood for semicrystalline than for amorphous polymers. Albeit some tendencies can be deduced (as disclosed) a reliable description is still missing. This is due to the strong interrelation between parameters of the crystalline structure [11,283] which does not allow us to study the effects of a given structural parameter separately. As a consequence, combined actions targeting the synthesis and in-depth characterization of polymers along with advanced "data mining" are required in order to close the gap between the toughness and structural parameters. A very straightforward approach is to detect the structural changes in situ during (e.g. [284]) or post mortem after the EWF test (e.g. [271,285]) by techniques with high spatial resolution.

List of symbols

E	[MPa]	Young's modulus
F	[N]	Tearing force of trousers specimen
F_s	[N]	saturation tearing force in Zone B (mode III loading)
H	[mm]	Height of the specimen
h	[mm]	Height of the outer plastic dissipation zone
h_B	[mm]	Fully developed plastic zone height in Zone B of trousers specimen
G_c	[kJ/m^2]	Strain energy release rate
J_c	[kJ/m^2]	J value for crack initiation
J_R	[-]	J resistance curve
K_c	[MPam$^{1/2}$]	Stress intensity factor
L	[mm]	Ligament length
L_a	[mm]	Length of the torn ligament in Zone A (mode III)
L_A	[mm]	Ligament length at the end of Zone A (mode III)
M_c	[g/mol]	Mean molecular weight between crosslinks
M_e	[g/mol]	Mean entanglement molecular weight
M_n	[g/mol]	Number-average molecular weight
M_Z	[g/mol]	Z-average molecular weight
m	[-]	Plastic flow constraint factor
r_p	[mm]	Radius of the plastic zone
T	[ºC]	Temperature
t	[mm]	Thickness of the specimen
u_d	[MJ/m^3]	Dissipative energy density
u_0	[kJ/m^2]	Limiting specific fracture energy
v	[mm/min]	Deformation rate
W	[mm]	Width of the specimen
W_e	[J]	Essential work of fracture
w_e	[kJ/m^2]	Specific essential work of fracture
w_{Ie}	[kJ/m^2]	Plane strain specific essential work of fracture
$w_{e,I}$	[kJ/m^2]	Specific essential work of fracture in Zone I (Initiation work-based energy partitioning)
$w_{e,II}$	[kJ/m^2]	Specific essential work of fracture in Zone II (Initiation work-based energy partitioning)
$w_{e,III}$	[kJ/m^2]	Specific essential work of fracture in mode III loading
$w_{e,y}$	[kJ/m^2]	Yielding-related specific essential work of fracture
$w_{e,n}$	[kJ/m^2]	Necking+tearing-related specific essential work of fracture
W_f	[J]	Total work of fracture
w_f	[kJ/m^2]	Specific total work of fracture
W_n	[J]	Work of fracture required for necking+tearing
w_n	[kJ/m^2]	Specific work of fracture required for necking+tearing
W_p	[J]	Non-essential or plastic work of fracture
w_p	[MJ/m^3]	Specific non-essential or plastic work of fracture
$w_{p,y}$	[MJ/m^3]	Specific yielding-related non-essential or plastic work of fracture
$w_{p,n}$	[MJ/m^3]	Specific necking+tearing-related non-essential or plastic work of fracture
$w_{p,I}$	[MJ/m^3]	Specific plastic work of fracture in Zone I (Initiation Work-based energy partitioning)
$w_{p,II}$	[MJ/m^3]	Specific plastic work of fracture in Zone II (Initiation Work-based energy partitioning)
w_{TE}	[kJ/m^2]	Specific tearing essential work of fracture in Zone A
w_{TE}^B	[kJ/m^2]	Specific tearing essential work of fracture in Zone B
w_{TF}	[kJ/m^2]	Specific tearing work of fracture in Zone A

w_{TF}^{B}	[kJ/m^2]	Specific tearing work of fracture in Zone B
w_{TP}	[MJ/m^3]	Specific tearing plastic work of fracture in Zone A
w_{TP}^{B}	[MJ/m^3]	Specific tearing plastic work of fracture in Zone B
W_y	[J]	Work of fracture required for yielding
w_y	[kJ/m^2]	Specific work of fracture required for yielding
W_I	[J]	Work of fracture required for irreversible initiation process involving yielding, necking and crack-tip blunting
W_{II}	[J]	Work of fracture required for crack propagation and extended necking in the plastic zone
w_I	[J]	Specific work of fracture required for irreversible initiation process involving yielding, necking and crack-tip blunting
w_{II}	[J]	Specific work of fracture required for crack propagation and extended necking in the plastic zone
x_0	[mm]	Extension derived from the intercept of x_b vs. L plot (equal to COD)
x_b	[mm]	Extension of specimen at failure
x_p	[mm]	Plastic contribution of extension derived from the intercept of x_b vs. L plot
α	[-]	Shape factor related to the tearing plastic work in Zone A
β	[-]	Shape factor related to the form of the outer plastic dissipation zone
Δa	[-]	Crack extension (J-integral)
σ_y	[MPa]	Uniaxial tensile yield stress
σ_n	[MPa]	Net section stress

List of abbreviations

AE	Acoustic emission
Al_2O_3	Aluminium oxide
aPP	Atactic polypropylene
ABS	Acrylonitrile butadiene styrene copolymer
$BaSO_4$	Barium sulphate
BOPET	Biaxially oriented polyethylene terephthalate
$CaCO_3$	Calcium carbonate (chalk)
CB	Carbon black
COD	Crack opening displacement
CPE	Chlorinated polyethylene
CTOD	Crack tip opening displacement
DEN-T	Double edge notched tensile (specimen)
DDEN-T	Deeply double edge notched tensile (specimen)
DSC	Differential scanning calorimetry
EP	Epoxy resin
EPBC	Ethylene propylene block copolymer
EPDM	Ethylene propylene diene rubber
EBA	Ethylene butylacrylate copolymer
EBR	Ethylene butylene copolymer (rubber)
EPR	Ethylene propylene rubber
EVA	Ethylene vinylacetate copolymer
EVOH	Ethylene vinylalcohol copolymer
EWF	Essential work of fracture method
EWIF	Essential work of interfacial fracture concept
FE	Finite element method
-g-	grafted by …
GB	Glass bead
GMA	Glycidyl methacrylate
HDPE	High density polyethylene

HIPS	High impact polystyrene
IFPZ	Inner fracture process zone
iPP	Isotactic polypropylene
LCP	Liquid crystalline polymer
LDH	Layered double hydroxides
LDPE	Low density polyethylene
LGF	Long glass fiber
LLDPE	Linear low density polyethylene
LNR	Liquid natural rubber
MA	Maleic anhydride
MFC	Microfibrillar composite
MW	Molecular weight
MWCNT	Multiwall carbon nanotube
NR	Natural rubber
OMMT	Organophilic modified montmorillonite
OPDZ	Outer process dissipation zone
POM	Polyoxymethylene
PA	Polyamide
PBT	Polybutylene terephthalate
PC	Polycarbonate
PCL	Polycaprolactone
PCTG	Polycyclohexane terephthalate glycol
PEEK	Polyether ether ketone
PEI	Polyether imide
PET	Polyethylene terephthalate
PETG	Polyethylene terephthalate glycol
PEN	Polyethylene naphthalate
phr	Parts per hundred parts resin
PI	Polyimide
POE	Polyoctene ethylene copolymer
PPT	Polypropylene terephthalate
PP	Polypropylene
PP-H	Polypropylene homopolymer
PP-BC	Polypropylene block copolymer
PPC	Polypropylene carbonate
PPE	Polyphenylene ether
PS	Polystyrene
PTFE	Polytetrafluoroethylene
PVC	Polyvinyl chloride
PU	Polyurethane
RT	Room temperature
RTPA	Rubber toughened polyamide
RTPP	Rubber toughened polypropylene
SAXS	Small angle X-ray scattering
SB	Styrene butadiene copolymer (star shaped)
SBS	Styrene butadiene styrene block copolymer
SEBS	Styrene ethylene butylene styrene
SEN-T	Single edge notched tensile (specimen)
SEN-B	Single edge notched bending (specimen)
SGF	Short glass fiber
SMA	Styrene maleic anhydride copolymer
TDV	Thermoplastic dynamic vulcanizate
TiO_2	Titanium dioxide

SiO_2 Silicon dioxide
sPP Syndiotactic polypropylene
uPVC Unplasticized polyvinylchloride
UHMWPE Ultra high molecular weight polyethylene
UV Ultraviolet irradiation

REFERENCES

[1] Broberg K. B.: Critical review of some theories in fracture mechanics. International Journal of Fracture, **4**, 11-18 (1968).
[2] Atkins A. G., Mai Y. W.: Elastic and Plastic Fracture. Ellis Horwood, Chichesters (1985).
[3] Williams J. G.: Fracture Mechanics of Polymer. Ellis Horwood, Chichesters (1987).
[4] Broberg K. B.: Crack-growth criteria and non-linear fracture mechanics. J Mech Phys Solids, **19**, 407-418 (1971).
[5] Broberg K. B.: On stable crack growth. J Mech Phys Solids, **23**, 215-237 (1975).
[6] Mai Y.-W., Wong S.-C., Chen X.-H.: Application of fracture mechanics for characterization of toughness of polymer blends. in 'Polymer Blends: Formulations and Performance' eds.: Paul D. R. and Bucknall C. B.) Wiley, New York, Vol 2, 17-58 (2000)
[7] Mai Y. W., Cotterell B.: The essential work of fracture for tearing of ductile metals. International Journal of Fracture, **24**, 229-236 (1984).
[8] Karger-Kocsis J.: Microstructural and molecular dependence of the work of fracture parameters in semicrystalline and amorphous polymer systems. in 'Fracture of Polymers, Composites and Adhesives' eds.: Williams J. G. and Pavan A.) Elsevier and ESIS Publ., Oxford, Vol 27, 213-230 (2000)
[9] Mai Y. W., Cotterell B.: On the essential work of ductile fracture in polymers. International Journal of Fracture, **32**, 105-125 (1986).
[10] Mai Y. W., Powell P.: Essential work of fracture and J-integral measurements for ductile polymers. Journal of Polymer Science Part B-Polymer Physics, **29**, 785-793 (1991).
[11] Karger-Kocsis J.: Fracture and fatigue behaviour of semicrystalline polymers as a function of microstructural and molecular parameters. in 'Structure Development During Polymer Processing' eds.: Cunha A. M. and Fakirov S.) Kluwer, Dordrecht, 163-179 (2000)
[12] Karger-Kocsis J.: For what kind of polymer is the toughness assessment by the essential work concept straightforward? Polymer Bulletin, **37**, 119-126 (1996).
[13] Hill R.: On discontinuous plastic states with special reference to localized necking in thin sheets. J Mech Phys Solids, **1**, 19-30 (1952).
[14] Mai Y. W., Cotterell B.: Effect of specimen geometry on the essential work of plane-stress ductile fracture. Engineering Fracture Mechanics, **21**, 123-128 (1985).
[15] Martinez A. B., Segovia A., Gamez-Perez J., Maspoch M. L.: Influence of femtolaser notch sharpening technique in the determination of essential work of fracture (EWF) parameters. Engineering Fracture Mechanics, **76**, 1247-1254 (2009).
[16] Gamez-Perez J., Santana O., Martinez A. B., Maspoch M. L.: Use of extensometers on essential work of fracture (EWF) tests. Polymer Testing, **27**, 491-497 (2008).
[17] Pegoretti A., Castellani L., Franchini L., Mariani P., Penati A.: On the essential work of fracture of linear low-density-polyethylene. I. Precision of the testing method. Engineering Fracture Mechanics, **76**, 2788-2798 (2009).
[18] Williams J. G., Rink M.: The standardisation of the EWF test. Engineering Fracture Mechanics, **74**, 1009-1017 (2007).
[19] Levita G., Parisi L., McLoughlin S.: Essential work of fracture in polymer films. Journal of Materials Science, **31**, 1545-1553 (1996).
[20] Saleemi A. S., Nairn J. A.: The plane-strain essential work of fracture as a measure of the fracture - toughness of ductile polymers. Polymer Engineering and Science, **30**, 211-218 (1990).

[21] Levita G., Parisi L., Marchetti A.: The work of fracture in semiductile polymers. Journal of Materials Science, **29**, 4545-4553 (1994).
[22] Karger-Kocsis J., Bárány T.: Plane-stress fracture behavior of syndiotactic polypropylenes of various crystallinity as assessed by the essential work of fracture method. Polymer Engineering and Science, **42**, 1410-1419 (2002).
[23] Martinez A. B., Gamez-Perez J., Sanchez-Soto M., Velasco J. I., Santana O. O., Maspoch M. L.: The essential work of fracture (EWF) method - Analyzing the post-yielding fracture mechanics of polymers. Engineering Failure Analysis, **16**, 2604-2617 (2009).
[24] Vu-Khanh T.: Impact fracture characterization of polymer with ductile behavior. Theoretical and Applied Fracture Mechanics, **21**, 83-90 (1994).
[25] Karger-Kocsis J., Moskala E. J.: Molecular dependence of the essential and non-essential work of fracture of amorphous films of poly(ethylene-2,6-naphthalate) (PEN). Polymer, **41**, 6301-6310 (2000).
[26] Mouzakis D. E., Karger-Kocsis J.: Essential work of fracture: application for polymers showing ductile-to-brittle transition during fracture. Polymer Bulletin, **42**, 473-480 (1999).
[27] Marchal Y., Walhin J. F., Delannay F.: Statistical procedure for improving the precision of the measurement of the essential work of fracture of thin sheets. International Journal of Fracture, **87**, 189-199 (1997).
[28] Karger-Kocsis J., Mouzakis D. E.: Effects of injection molding-induced morphology on the work of fracture parameters in rubber-toughened polypropylenes. Polymer Engineering and Science, **39**, 1365-1374 (1999).
[29] Sova M., Raab M., Slizova M.: Polypropylene composite materials oriented by solid-state drawing - low temperature impact behavior. Journal of Materials Science, **28**, 6516-6523 (1993).
[30] Clutton E.: Microstructural and molecular dependence of the work of fracture parameters in semicrystalline and amorphous polymer systems. in 'Fracture Mechanics Testing Methods for Polymers, Adhesives and Composites' eds.: Moore D. R. and Pavan A. and Williams J. G.) Elsevier and ESIS Publ., Oxford, Vol 28, 177-195 (2001)
[31] 2004.
[32] Ramsteiner F., Schuster W., Forster S.: Concepts of fracture mechanics for polymers. in 'Deformation and Fracture Behaviour of Polymers' eds.: Grellmann W. and Seidler S.) Springer, Berlin, 27-50 (2001)
[33] Casellas J. J., Frontini P. M., Carella J. M.: Fracture characterization of low-density polyethylenes by the essential work of fracture: Changes induced by thermal treatments and testing temperature. Journal of Applied Polymer Science, **74**, 781-796 (1999).
[34] Yang W., Shan G. F., Tang X. G., Xie B. H., Li Z. M., Zhou Q. C., Yang M. B.: Structures and properties of blown moulding LLDPE films. Plastics Rubber and Composites, **35**, 368-374 (2006).
[35] Chan W. Y. F., Williams J. G.: Determination of the fracture-toughness of polymeric films by the essential work method. Polymer, **35**, 1666-1672 (1994).
[36] Wu J. S., Mai Y. W.: The essential fracture work concept for toughness measurement of ductile polymers. Polymer Engineering and Science, **36**, 2275-2288 (1996).
[37] Na B., Lv R. H.: Relationship between fracture toughness and intrinsic deformation parameters in isotropic and flow-oriented linear low-density polyethylene. Journal of Polymer Science Part B-Polymer Physics, **44**, 2880-2887 (2006).
[38] Peres F. M., Schon C. G.: Application of the essential work of fracture method in ranking the performance in service of high-density polyethylene resins employed in pressure pipes. Journal of Materials Science, **43**, 1844-1850 (2008).
[39] Kwon H. J., Jar R. Y. B.: Application of essential work of fracture concept to toughness characterization of high-density polyethylene. Polymer Engineering and Science, **47**, 1327-1337 (2007).
[40] Ferrer-Balas D., Maspoch M. L., Martinez A. B., Santana O. O.: On the essential work of fracture method: Energy partitioning of the fracture process in iPP films. Polymer Bulletin, **42**, 101-108 (1999).

[41] Gamez-Perez J., Santana O. O., Gordillo A., Maspoch M. L.: Evaluation of the fracture behavior of multilayered polypropylene sheets obtained by coextrusion. Polymer Engineering and Science, **47**, 1365-1372 (2007).
[42] Pegoretti A., Marchi A., Ricco T.: Determination of the fracture toughness of thermoformed polypropylene cups by the essential work method. Polymer Engineering and Science, **37**, 1045-1052 (1997).
[43] Na B., Lv R. H.: Effect of cavitation on the plastic deformation and failure of isotactic polypropylene. Journal of Applied Polymer Science, **105**, 3274-3279 (2007).
[44] Fayolle B., Audouin L., Verdu J.: Initial steps and embrittlement in the thermal oxidation of stabilised polypropylene films. Polymer Degradation and Stability, **75**, 123-129 (2002).
[45] Fayolle B., Tcharkhtchi A., Verdu J.: Temperature and molecular weight dependence of fracture behaviour of polypropylene films. Polymer Testing, **23**, 939-947 (2004).
[46] Mohanraj J., Chapleau N., Ajji A., Duckett R. A., Ward I. M.: Fracture behavior of die-drawn toughened polypropylenes. Journal of Applied Polymer Science, **88**, 1336-1345 (2003).
[47] Grein C., Plummer C. J. G., Germain Y., Kausch H. H., Beguelin P.: Essential work of fracture of polypropylene and polypropylene blends over a wide range of test speeds. Polymer Engineering and Science, **43**, 223-233 (2003).
[48] Ferrer-Balas D., Maspoch M. L., Mai Y. W.: Fracture behaviour of polypropylene films at different temperatures: fractography and deformation mechanisms studied by SEM. Polymer, **43**, 3083-3091 (2002).
[49] Ferrer-Balas D., Maspoch M. L., Martinez A. B., Ching E., Li R. K. Y., Mai Y. W.: Fracture behaviour of polypropylene films at different temperatures: assessment of the EWF parameters. Polymer, **42**, 2665-2674 (2001).
[50] Ferrer-Balas D., Maspoch M. L., Martinez A. B., Santana O. O.: Influence of annealing on the microstructural, tensile and fracture properties of polypropylene films. Polymer, **42**, 1697-1705 (2001).
[51] Maspoch M. L., Ferrer D., Gordillo A., Santana O. O., Martinez A. B.: Effect of the specimen dimensions and the test speed on the fracture toughness of iPP by the essential work of fracture (EWF) method. Journal of Applied Polymer Science, **73**, 177-187 (1999).
[52] Bohaty P., Vlach B., Seidler S., Koch T., Nezbedova E.: Essential work of fracture and the phase transformation in beta-iPP. Journal of Macromolecular Science-Physics, **B41**, 657-669 (2002).
[53] Tordjeman P., Robert C., Marin G., Gerard P.: The effect of alpha, beta crystalline structure on the mechanical properties of polypropylene. European Physical Journal E, **4**, 459-465 (2001).
[54] Karger-Kocsis J., Varga J.: Effects of beta-alpha transformation on the static and dynamic tensile behavior of isotactic polypropylene. Journal of Applied Polymer Science, **62**, 291-300 (1996).
[55] Karger-Kocsis J.: How does "phase transformation toughening" work in semicrystalline polymers? Polymer Engineering and Science, **36**, 203-210 (1996).
[56] Lv R. H., Xu W. F., Na B., Yan J. Z.: Correlation of mechanical behaviors with crystalline phase and related cavitation in isotactic polypropylene. Journal of Applied Polymer Science, **108**, 3185-3190 (2008).
[57] Sheng B. R., Li B., Xie B. H., Yang W., Feng H. M., Yang M. B.: Influences of molecular weight and crystalline structure on fracture behavior of controlled-rheology-polypropylene prepared by reactive extrusion. Polymer Degradation and Stability, **93**, 225-232 (2008).
[58] Li Q. G., Xie B. H., Yang W., Li Z. M., Zhang W. Q., Yang M. B.: Effect of annealing on fracture behavior of poly(propylene-block-ethylene) using essential work of fracture analysis. Journal of Applied Polymer Science, **103**, 3438-3446 (2007).
[59] Maspoch M. L., Gamez-Perez J., Gordillo A., Sanchez-Soto M., Velasco J. I.: Characterisation of injected EPBC plaques using the essential work of fracture (EWF) method. Polymer, **43**, 4177-4183 (2002).
[60] Gamez-Perez J., Munoz P., Santana O. O., Gordillo A., Maspoch M. L.: Influence of processing on ethylene propylene block copolymers (II): Fracture behavior. Journal of Applied Polymer Science, **101**, 2714-2724 (2006).

[61] Gamez-Perez J., Munoz P., Velasco J. I., Martinez A. B., Maspoch M. L.: Determination of essential work of fracture in EPBC sheets obtained by different transformation processes. Journal of Materials Science, **40**, 1967-1974 (2005).
[62] Wang S. W., Yang W., Gong G., Xie B. H., Liu Z. Y., Yang M. B.: Effect of alpha- and beta-nucleating agents on the fracture behavior of polypropylene-co-ethylene. Journal of Applied Polymer Science, **108**, 591-597 (2008).
[63] Mouzakis D. E., Gahleitner M., Karger-Kocsis J.: Toughness assessment of elastomeric polypropylene (ELPP) by the essential work of the fracture method. Journal of Applied Polymer Science, **70**, 873-881 (1998).
[64] Karger-Kocsis J.: Toward understanding the morphology-related crack initiation and propagation behavior in polypropylene systems as assessed by the essential work of fracture approach. Journal of Macromolecular Science-Physics, **B38**, 635-646 (1999).
[65] Bárány T., Földes E., Czigány T., Karger-Kocsis J.: Effect of UV aging on the tensile and fracture mechanical response of syndiotactic polypropylenes of various crystallinity. Journal of Applied Polymer Science, **91**, 3462-3469 (2004).
[66] Fung K. L., Zhao H. X., Wang J. T., Meng Y. Z., Tjong S. C., Li R. K. Y.: Essential work of fracture (EWF) analysis for compression molded alternating poly(propylene carbonate). Polymer Engineering and Science, **44**, 580-587 (2004).
[67] Wang X. L., Li R. K. Y., Cao Y. X., Meng Y. Z.: Essential work of fracture analysis of poly(propylene carbonate) with varying molecular weight. Polymer Testing, **24**, 699-703 (2005).
[68] Kuno T., Yamagishi Y., Kawamura T., Nitta K.: Deformation mechanism under essential work of fracture process in polycyclo-olefin materials. Express Polymer Letters, **2**, 404-412 (2008).
[69] Hashemi S.: Work of fracture of high impact polystyrene (HIPS) film under plane stress conditions. Journal of Materials Science, **38**, 3055-3062 (2003).
[70] Luna P., Bernal C., Cisilino A., Frontini P., Cotterell B., Mai Y. W.: The application of the essential work of fracture methodology to the plane strain fracture of ABS 3-point bend specimens. Polymer, **44**, 1145-1150 (2003).
[71] Lau S. W., Truss R. W.: The essential work of fracture through the wall of a uPVC pipe. Journal of Materials Science, **37**, 1115-1119 (2002).
[72] Kwon J. A., Truss R. W.: The work of fracture in uniaxial and biaxial oriented unplasticised polyvinylchloride pipes. Engineering Fracture Mechanics, **69**, 605-616 (2002).
[73] Levita G., Parisi L., Marchetti A., Bartolommei L.: Effects of thickness on the specific essential work of fracture of rigid PVC. Polymer Engineering and Science, **36**, 2534-2541 (1996).
[74] Arkhireyeva A., Hashemi S., O'Brien M.: Factors affecting work of fracture of uPVC film. Journal of Materials Science, **34**, 5961-5974 (1999).
[75] Arkhireyeva A., Hashemi S.: Combined effect of temperature and thickness on work of fracture parameters of unplasticized PVC film. Polymer Engineering and Science, **42**, 504-518 (2002).
[76] Maspoch M. L., Gamez-Perez J., Karger-Kocsis J.: Effects of thickness, deformation rate and energy partitioning on the work of fracture parameters of uPVC films. Polymer Bulletin, **50**, 279-286 (2003).
[77] Wallner G. M., Major Z., Maier G., Lang R. W.: Influence of annealing on the fracture behavior of 200 mu m thick alpha-PVDF films. Advanced Engineering Materials, **8**, 1140-1145 (2006).
[78] Wallner G. M., Major Z., Maier G. A., Lang R. W.: Fracture analysis of annealed PVDF films. Polymer Testing, **27**, 392-402 (2008).
[79] Plummer C. J. G., Scaramuzzino P., Steinberger R., Lang R. W., Kausch H. H.: Application of the essential work of fracture concept to high temperature deformation in polyoxymethylene. Polymer Engineering and Science, **40**, 985-991 (2000).
[80] Yamakawa R. S., Razzino C. A., Correa C. A., Hage E.: Influence of notching and molding conditions on determination of EWF parameters in polyamide 6. Polymer Testing, **23**, 195-202 (2004).
[81] Pegoretti A., Ricco T.: On the essential work of fracture of neat and rubber toughened polyamide-66. Engineering Fracture Mechanics, **73**, 2486-2502 (2006).

[82] Arkhireyeva A., Hashemi S.: Determination of fracture toughness of poly(ethylene terephthalate) film by essential work of fracture and J integral measurements. Plastics Rubber and Composites, **30**, 337-350 (2001).
[83] Arkhireyeva A., Hashemi S.: Influence of temperature on plane stress ductile fracture of poly(ethylene terephthalate) film. Plastics Rubber and Composites, **30**, 125-131 (2001).
[84] Hashemi S., Arkhireyeva A.: Influence of temperature on work of fracture parameters in semi-crystalline polyester films. Journal of Macromolecular Science-Physics, **B41**, 863-880 (2002).
[85] Hashemi S.: Fracture toughness evaluation of ductile polymeric films. Journal of Materials Science, **32**, 1563-1573 (1997).
[86] Maspoch M. L., Henault V., Ferrer-Balas D., Velasco J. I., Santana O. O.: Essential work of fracture on PET films: influence of the thickness and the orientation. Polymer Testing, **19**, 559-568 (2000).
[87] Light M. E., Lesser A. J.: Effect of test conditions on the essential work of fracture in polyethylene terephthalate film. Journal of Materials Science, **40**, 2861-2866 (2005).
[88] Hashemi S., Xu Y.: Thermal effects on fracture of biaxial-oriented poly(ethylene terephthalate) (BOPET) film. Journal of Materials Science, **42**, 6197-6204 (2007).
[89] Karger-Kocsis J., Czigány T.: On the essential and non-essential work of fracture of biaxial-oriented filled PET film. Polymer, **37**, 2433-2438 (1996).
[90] Arkhireyeva A., Hashemi S.: Effect of temperature on fracture properties of an amorphous poly(ethylene terephthalate) (PET) film. Journal of Materials Science, **37**, 3675-3683 (2002).
[91] Bárány T., Karger-Kocsis J., Czigány T.: Effect of hygrothermal aging on the essential work of fracture response of amorphous poly(ethylene terephthalate) sheets. Polymer Degradation and Stability, **82**, 271-278 (2003).
[92] Vincent L., Connolly S. N., Dolan F., Willcocks P. H., Jayaweera S. A. A., Pendlebury R.: Determination and comparison of the plane stress essential work of fracture of three polyesters PET, PPT and PBT. Journal of Thermal Analysis and Calorimetry, **86**, 147-154 (2006).
[93] Bárány T., Földes E., Czigány T.: Effect of thermal and hygrothermal aging on the plane stress fracture toughness of poly(ethylene terephthalate) sheets. Express Polymer Letters, **1**, 180-187 (2007).
[94] Bárány T., Ronkay F., Karger-Kocsis J., Czigány T.: In-plane and out-of-plane fracture toughness of physically aged polyesters as assessed by the essential work of fracture (EWF) method. International Journal of Fracture, **135**, 251-265 (2005).
[95] Ching E. C. Y., Li R. K. Y., Mai Y. W.: Effects of gauge length and strain rate on fracture toughness of polyethylene terephthalate glycol (PETG) film using the Essential Work of Fracture analysis. Polymer Engineering and Science, **40**, 310-319 (2000).
[96] Pascual A. L., Beeman C. S., Hicks E. P., Bush H. M., Mitchell R. J.: The essential work of fracture of thermoplastic orthodontic retainer materials. Angle Orthodontist, **80**, 554-560 (2010).
[97] Poon W. K. Y., Ching E. C. Y., Cheng C. Y., Li R. K. Y.: Measurement of plane stress essential work of fracture (EWF) for polymer films: effects of gripping and notching methodology. Polymer Testing, **20**, 395-401 (2001).
[98] Karger-Kocsis J., Bárány T., Moskala E. J.: Plane stress fracture toughness of physically aged plasticized PETG as assessed by the essential work of fracture (EWF) method. Polymer, **44**, 5691-5699 (2003).
[99] Karger-Kocsis J., Czigány T., Moskala E. J.: Deformation rate dependence of the essential and non-essential work of fracture parameters in an amorphous copolyester. Polymer, **39**, 3939-3944 (1998).
[100] Karger-Kocsis J., Czigány T., Moskala E. J.: Thickness dependence of work of fracture parameters of an amorphous copolyester. Polymer, **38**, 4587-4593 (1997).
[101] Liu C. H., Nairn J. A.: Using the essential work of fracture method for studying physical aging in thin, ductile, polymeric films. Polymer Engineering and Science, **38**, 186-193 (1998).
[102] Mouzakis D. E., Karger-Kocsis J., Moskala E. J.: Interrelation between energy partitioned work of fracture parameters and the crack tip opening displacement in amorphous polyester films. Journal of Materials Science Letters, **19**, 1615-1619 (2000).

[103] Karger-Kocsis J., Moskala E. J.: Relationships between molecular and plane-stress essential work of fracture parameters in amorphous copolyesters. Polymer Bulletin, **39**, 503-510 (1997).
[104] Chen H. B., Karger-Kocsis J., Wu J. S.: Effects of molecular structure on the essential work of fracture of amorphous copolyesters at various deformation rates. Polymer, **45**, 6375-6382 (2004).
[105] Hashemi S.: Temperature dependence of work of fracture parameters in polybutylene terephthalate (PBT). Polymer Engineering and Science, **40**, 1435-1446 (2000).
[106] Hashemi S.: Deformation rate dependence of work of fracture parameters in polybutylene terephthalate (PBT). Polymer Engineering and Science, **40**, 132-138 (2000).
[107] Hashemi S.: Determination of the fracture toughness of polybutylene terephthalate (PBT) film by the essential work method: Effect of specimen size and geometry. Polymer Engineering and Science, **40**, 798-808 (2000).
[108] Hashemi S.: Fracture of polybutylene terephthalate (PBT) film. Polymer, **43**, 4033-4041 (2002).
[109] Arkhireyeva A., Hashemi S.: Fracture behaviour of polyethylene naphthalate (PEN). Polymer, **43**, 289-300 (2002).
[110] Karger-Kocsis J., Czigány T.: Strain rate dependence of the work of fracture response of an amorphous poly(ethylene-naphthalate) (PEN) film. Polymer Engineering and Science, **40**, 1809-1815 (2000).
[111] Maspoch M. L., Santana O. O., Grando J., Ferrer D., Martinez A. B.: The essential work of fracture of a thermoplastic elastomer. Polymer Bulletin, **39**, 249-255 (1997).
[112] Lee J. M., Choi B. H., Moon J. S., Lee E. S.: Determination of the tear properties of thermoplastic polyester elastomers (TPEEs) using essential work of fracture (EWF) test method. Polymer Testing, **28**, 854-865 (2009).
[113] Hashemi S.: Plane-stress fracture of polycarbonate films. Journal of Materials Science, **28**, 6178-6184 (1993).
[114] Hashemi S.: Temperature and deformation rate dependence of the work of fracture in polycarbonate (PC) film. Journal of Materials Science, **35**, 5851-5856 (2000).
[115] Hashemi S., Williams J. G.: Temperature dependence of essential and non-essential work of fracture parameters for polycarbonate film. Plastics Rubber and Composites, **29**, 294-302 (2000).
[116] Ho C. H., Vu-Khanh T.: Physical aging and time-temperature behavior concerning fracture performance of polycarbonate. Theoretical and Applied Fracture Mechanics, **41**, 103-114 (2004).
[117] Paton C. A., Hashemi S.: Plane-stress essential work of ductile fracture for polycarbonate. Journal of Materials Science, **27**, 2279-2290 (1992).
[118] Arkhireyeva A., Hashemi S.: Effect of temperature on work of fracture parameters in poly(ether-ether ketone) (PEEK) film. Engineering Fracture Mechanics, **71**, 789-804 (2004).
[119] Hashemi S.: Effect of temperature on fracture toughness of an amorphous poly(ether-ether ketone) film using essential work of fracture analysis. Polymer Testing, **22**, 589-599 (2003).
[120] Hashemi S., Obrien D.: The essential work of plane-stress ductile fracture of poly(ether-ether ketone) thermoplastic. Journal of Materials Science, **28**, 3977-3982 (1993).
[121] Zhao H. X., Li R. K. Y.: Fracture behaviour of poly(ether ether ketone) films with different thicknesses. Mechanics of Materials, **38**, 100-110 (2006).
[122] Chen H. B., Wu J. S.: Understanding the underlying physics of the essential work of fracture on the molecular level. Macromolecules, **40**, 4322-4326 (2007).
[123] Chen H. B., Wu J. S.: Specific essential work of fracture of polyurethane thin films with different molecular structures. Journal of Polymer Science Part B-Polymer Physics, **45**, 1418-1424 (2007).
[124] Fayolle B., Verdu J.: EWF method to study long term fracture properties of cross-linked polyethylene. Polymer Engineering and Science, **45**, 424-431 (2005).
[125] Lesser A. J., Jones N. A.: Fracture behavior of dynamically vulcanized thermoplastic elastomers. Journal of Applied Polymer Science, **76**, 763-770 (2000).
[126] Shen Y. X., Xie B. H., Yang W., Li Z. M., Yang M. B.: Effect of EPDM content on melt flow, microstructures and fracture behavior of dynamically vulcanized PP/EPDM blends. Journal of Macromolecular Science Part B-Physics, **46**, 1127-1138 (2007).

[127] Tang X. G., Bao R. Y., Yang W., Xie B. H., Yang M. B., Hou M.: Effect of beta-phase on the fracture behavior of dynamically vulcanized PP/EPDM blends studied by the essential work of fracture approach. European Polymer Journal, **45**, 1448-1453 (2009).
[128] Hernandez M., Santana O. O., Ichazo M. N., Gonzalez J., Albano C.: Fracture behavior at low strain rate of dynamically and statically vulcanized polypropylene/styrene-butadiene-styrene block copolymer blends. Polymer Testing, **27**, 881-885 (2008).
[129] Pfaff F. A.: Growing more ductile epoxies: an essential work of fracture study. Journal of Coatings Technology and Research, **4**, 151-159 (2007).
[130] Zhang Z., Evans D.: Investigation of fracture properties of epoxy at low temperatures. Polymer Engineering and Science, **43**, 1071-1080 (2003).
[131] Singh S. K., Tambe S. P., Kumar D.: Effect of pigmentation on fracture toughness of paint films. Journal of Materials Science, **39**, 2629-2632 (2004).
[132] Lee J., Macosko C. W., Urry D. W.: Mechanical properties of cross-linked synthetic elastomeric polypentapeptides. Macromolecules, **34**, 5968-5974 (2001).
[133] Chaleat C. M., Halley P. J., Truss R. W.: Properties of a plasticised starch blend. Part 1: Influence of moisture content on fracture properties. Carbohydrate Polymers, **71**, 535-543 (2008).
[134] Yakimets I., Wellner N., Smith A. C., Wilson R. H., Farhat I., Mitchell J.: Effect of water content on the fracture behaviour of hydroxypropyl cellulose films studied by the essential work of fracture method. Mechanics of Materials, **39**, 500-512 (2007).
[135] Plucknett K. P., Normand V.: Plane stress essential work of fracture of 'pseudo-ductile' gelatin/maltodextrin biopolymer gel composites. Polymer, **41**, 6833-6841 (2000).
[136] Na B., Lv R. H., Zhao Z. X.: Dispersed microfibril-dominated deformation and fracture behaviors of linear low density polyethylene/isotactic polypropylene blends. Journal of Applied Polymer Science, **104**, 1291-1298 (2007).
[137] Fasce L., Chiaverano G., Lach R., Frontini P.: Essential work of fracture of photo-oxidized LDPE/EVA films. Macromolecular Symposia, **247**, 271-281 (2007).
[138] Tjong S. C., Xu S. A., Li R. K. Y.: Work of fracture of polystyrene/high density polyethylene blends compatibilized by triblock copolymer. Journal of Applied Polymer Science, **77**, 2074-2081 (2000).
[139] Supatham P., Tabtiang A., Venables R. A.: Plane stress fracture toughness of partially miscible, high-density polyethylene/poly (ethylene-co-1-octene) blends. Polymer-Plastics Technology and Engineering, **44**, 363-379 (2005).
[140] Marchal Y., Oldenhove B., Daoust D., Legras R., Delannay F.: Characterization of the fracture toughness of rubber-toughened polypropylene thin plates. Polymer Engineering and Science, **38**, 2063-2071 (1998).
[141] Yokoyama Y., Ricco T.: Toughening of polypropylene by different elastomeric systems. Polymer, **39**, 3675-3681 (1998).
[142] Mouzakis D. E., Mader D., Mulhaupt R., Karger-Kocsis J.: Relationship between morphology and mechanical properties of polypropylene/ethene-co-butene binary blends with various butene contents. Journal of Materials Science, **35**, 1219-1230 (2000).
[143] Li W. D., Li R. K. Y., Tjong S. C.: Fracture toughness of elastomer-modified polypropylene. Polymer Testing, **16**, 563-574 (1997).
[144] Khodabandelou M., Aghjeh M. K. R., Rezaei M.: Fracture behavior and environmental stress cracking resistance (ESCR) of HIPS/PE blends and the effect of compatibilization on their properties. Engineering Fracture Mechanics, **76**, 2856-2867 (2009).
[145] Lach R., Weidisch R., Janke A., Knoll K.: Influence of domain size on toughness of poly(styrene-block-butadiene) star block copolymer/polystyrene blends. Macromolecular Rapid Communications, **25**, 2019-2024 (2004).
[146] Liu Y., Xie B. H., Yang W., Zhang W. Q., Feng J. M., Yang M. B.: Morphology and fracture behaviour of poly(vinyl chloride)/ethylene-vinyl acetate copolymer blends. Polymer Testing, **26**, 388-395 (2007).
[147] Whittle A. J., Burford R. P., Hoffman M. J.: Assessment of strength and toughness of modified PVC pipes. Plastics Rubber and Composites, **30**, 434-440 (2001).

[148] Heino M., Hietaoja P., Seppala J., Harmia T., Friedrich K.: Studies on fracture behavior of tough PA6/PP blends. Journal of Applied Polymer Science, **66**, 2209-2220 (1997).
[149] Balamurugan G. P., Maiti S. N.: The influence of reactive compatibilization on uniaxial large strain deformation and fracture behavior of polyamide 6 and poly(ethylene-co-butyl acrylate) blends. Polymer Testing, **27**, 752-764 (2008).
[150] Jing B., Dai W., Liu P., Zhang P.: Fracture toughness evaluation of K resin (R) grafted with maleic anhydride compatibilized polyamide-6/K-resin (R) blends. Polymer International, **56**, 1240-1246 (2007).
[151] Pisharath S., Wong S. C., Hu X.: Fracture behavior of nylon hybrid composites. Journal of Materials Science, **39**, 6529-6538 (2004).
[152] Fung K. L., Li R. K. Y.: A study on the fracture characteristics of rubber toughened poly(ethylene terephthalate) blends. Polymer Testing, **24**, 863-872 (2005).
[153] Mouzakis D. E., Papke N., Wu J. S., Karger-Kocsis J.: Fracture toughness assessment of poly(ethylene terephthalate) blends with glycidyl methacrylate modified polyolefin elastomer using essential work of fracture method. Journal of Applied Polymer Science, **79**, 842-852 (2001).
[154] Billon N., Meyer J.-P.: Experimantal studz of rubber-toughening of PET. in 'Fracture of Polymers, Composites and Adhesives II,' eds.: Blackman B. R. K. and Pavan A. and Williams J. G.) Elsevier Ltd. and ESIS, Oxford, Vol 32, 65-75 (2003)
[155] Sanchez J. J., Santana O., Gordillo A., Maspoch M. L., Martinez A. B.: Essential work of fracture of injection moulded samples of PET and PET/PC blends. in 'Fracture of Polymers, Composites and Adhesives II,' eds.: Blackman B. R. K. and Pavan A. and Williams J. G.) Elsevier Ltd. and ESIS, Oxford, Vol 32, 77-88 (2003)
[156] Vincent L., Connolly S. N., Dolan F., Willcocks P. H., Jayaweera S. A. A.: Determination and comparison of the essential work of fracture (EWF) of two polyester blends. Journal of Thermal Analysis and Calorimetry, **86**, 155-164 (2006).
[157] Hashemi S.: Work of fracture of PBT/PC blend: Effect of specimen size, geometry, and rate of testing. Polymer Engineering and Science, **37**, 912-921 (1997).
[158] Wu J. S., Mai Y. W., Cotterell B.: Fracture-toughness and fracture mechanisms of PBT/PC/IM blend. 2. Fracture properties. Journal of Materials Science, **28**, 3373-3384 (1993).
[159] Jing B., Dai W. L., Chen S. B., Hu T., Liu P. S.: Mechanical behavior and fracture toughness evaluation of K resin grafted with maleic anhydride compatibilized polycarbonate/K resin blends. Materials Science and Engineering a-Structural Materials Properties Microstructure and Processing, **444**, 84-91 (2007).
[160] Yang W., Xie B. H., Shi W., Li Z. M., Liu Z. Y., Chen J., Yang M. B.: Essential work of fracture evaluation of fracture behavior of glass bead filled linear low-density polyethylene. Journal of Applied Polymer Science, **99**, 1781-1787 (2006).
[161] Yang W., Xie B. H., Shi W., Zuo M., Li Z. M., Yang M. B.: Essential work of fracture of glass bead filled low density polyethylene. Journal of Materials Science, **40**, 5323-5326 (2005).
[162] Wetherhold R. C., Mouzakis D. E.: Fracture behavior of kaolin-reinforced high density polyethylene. Journal of Engineering Materials and Technology-Transactions of the Asme, **121**, 483-487 (1999).
[163] Wetherhold R. C., Mouzakis D. E., Friedrich K.: Effects of testing speed and heat treatment on the fracture of kaolin-reinforced high density polyethylene. Journal of Materials Science Letters, **19**, 179-182 (2000).
[164] Li Z. M., Xie B. H., Huang R., Fang M. P., Yang M.: Influences of hot stretch ratio on essential work of fracture of in-situ microfibrillar poly(ethylene terephthalate)/polyethylene blends. Polymer Engineering and Science, **44**, 2165-2173 (2004).
[165] Li Z. M., Yang W., Huang R., Fang X. P., Yang M. B.: Essential work of fracture parameters of in-situ microfibrillar poly(ethylene terephthalate)/polyethylene blend: Influences of blend composition. Macromolecular Materials and Engineering, **289**, 426-433 (2004).
[166] Li Z. M., Yang W., Xie B. H., Yang S. Y., Yang M. B., Feng J. M., Rui H. A.: Effects of compatibilization on the essential work of fracture parameters of in situ microfiber reinforced

poly(ethylene terephtahalate)/polyethylene blend. Materials Research Bulletin, **38**, 1867-1878 (2003).
[167] Wang K., Wu J. S., Zeng H. M.: Microstructure and fracture behavior of polypropylene/barium sulfate composites. Journal of Applied Polymer Science, **99**, 1207-1213 (2006).
[168] Gong G., Xie B. H., Yang W., Li Z. M., Lai S. M., Yang M. B.: Plastic deformation behavior of polypropylene/calcium carbonate composites with and without maleic anhydride grafted polypropylene incorporated using the essential work of fracture method. Polymer Testing, **25**, 98-106 (2006).
[169] Gong G., Xie B. H., Yang W., Li Z. M., Zhang W. Q., Yang M. B.: Essential work of fracture (EWF) analysis for polypropylene grafted with maleic anhydride modified polypropylene/calcium carbonate composites. Polymer Testing, **24**, 410-417 (2005).
[170] Mouzakis D. E., Stricker F., Mulhaupt R., Karger-Kocsis J.: Fracture behaviour of polypropylene/glass bead elastomer composites by using the essential work-of-fracture method. Journal of Materials Science, **33**, 2551-2562 (1998).
[171] Tjong S. C., Xu S. A., Li R. K. Y., Mai Y. W.: Mechanical behavior and fracture toughness evaluation of maleic anhydride compatibilized short glass fiber/SEBS/polypropylene hybrid composites. Composites Science and Technology, **62**, 831-840 (2002).
[172] Tjong S. C., Xu S. A., Li R. K. Y., Mai Y. W.: Fracture characteristics of short glass fibre/maleated styrene-ethylene-butylene-styrene/polypropylene hybrid composite. Polymer International, **51**, 1248-1255 (2002).
[173] Tjong S. C., Xu S. A., Li R. K. Y., Mai Y. W.: Tensile deformation mechanisms of polypropylene/elastomer blends reinforced with short glass fiber. Journal of Applied Polymer Science, **87**, 441-451 (2003).
[174] Mouzakis D. E., Harmia T., Karger-Kocsis J.: Fracture behaviour of discontinuous long glass fibre reinforced injection moulded polypropylene. Polymers & Polymer Composites, **8**, 167-175 (2000).
[175] Gong G., Xie B. H., Yang M. B., Yang W., Zhang W. Q., Zhao M.: Mechanical properties and fracture behavior of injection and compression molded polypropylene/coal gangue powder composites with and without a polymeric coupling agent. Composites Part a-Applied Science and Manufacturing, **38**, 1683-1693 (2007).
[176] Li B., Gong G., Xie B. H., Yang W., Yang M. B., Lai S. M.: Fracture behaviour of polypropylene sheets filled with epoxidized natural rubber (ENR)-treated coal gangue powder. Journal of Materials Science, **42**, 3856-3864 (2007).
[177] Liu Y., Xie B. H., Yang W., Yang M. B.: The Composition, Morphology, and Mechanical Properties of Ethylene Propylene Diene Monomer-Encapsulated Coal Gangue Powder/Polypropylene Composites. Polymer Composites, **31**, 10-17 (2010).
[178] Anuar H., Ahmad S. H., Rasid R., Surip S. N., Czigány T., Romhány G.: Essential work of fracture and acoustic emission study on TPNR composites reinforced by kenaf fiber. Journal of Composite Materials, **41**, 3035-3049 (2007).
[179] Arencon D., Velasco J. I., Realinho V., Antunes M., Maspoch M. L.: Essential work of fracture analysis of glass micro sphere-filled polypropylene and polypropylene/poly (ethylene terephthalateco-isophthalate) blend-matrix composites. Polymer Testing, **26**, 761-769 (2007).
[180] Arencon D., Velasco J. I.: Tensile behaviour and fracture toughness of EPDM filled with untreated and silane-treated glass beads. Journal of Materials Science, **36**, 179-187 (2001).
[181] Wong S. C., Mai Y. W.: Essential fracture work of short fiber reinforced polymer blends. Polymer Engineering and Science, **39**, 356-364 (1999).
[182] Tjong S. C., Xu S. A., Li R. K. Y., Mai Y. W.: Short glass fiber-reinforced polyamide 6,6 composites toughened with maleated SEBS. Composites Science and Technology, **62**, 2017-2027 (2002).
[183] Ching E. C. Y., Li R. K. Y., Tjong S. C., Mai Y. W.: Essential work of fracture (EWF) analysis for short glass fiber reinforced and rubber toughened nylon-6. Polymer Engineering and Science, **43**, 558-569 (2003).

[184] Sui G. X., Wong S. C., Yue C. Y.: The effect of fiber inclusions in toughened plastics - part I: Fracture characterization by essential fracture work. Composites Science and Technology, **61**, 2481-2490 (2001).
[185] Sui G. X., Wong S. C., Yue C. Y.: Effect of extrusion compounding on the mechanical properties of rubber-toughened polymers containing short glass fibers. Journal of Materials Processing Technology, **113**, 167-171 (2001).
[186] Wong S. C., Sui G. X., Yue C. Y., Mai Y. W.: Characterization of microstructures and toughening behavior of fiber-containing toughened nylon 6,6. Journal of Materials Science, **37**, 2659-2667 (2002).
[187] Wang X. L., Li R. Y., Cao Y. X., Meng Y. Z.: Essential work of fracture analysis for starch filled poly(propylene carbonate) composites. Materials & Design, **28**, 1934-1939 (2007).
[188] Williams M. A., Bauman B. D., Thomas D. A.: Incorporation of surface-modified UHMWPE powders and fibers in tough polyurethane composites. Polymer Engineering and Science, **31**, 992-998 (1991).
[189] Wong S. C., Baji A., Gent A. N.: Effect of specimen thickness on fracture toughness and adhesive properties of hydroxyapatite-filled polycaprolactone. Composites Part a-Applied Science and Manufacturing, **39**, 579-587 (2008).
[190] Vu H. N., Vermogen A., Gauthier C., Masenelli-Varlot K., Cavaille J. Y.: Microstructure and fracture behavior of semicrystalline polymer-clay nanocomposites. Journal of Polymer Science Part B-Polymer Physics, **46**, 1820-1836 (2008).
[191] Costa F. R., Satapathy B. K., Wagenknecht U., Weidisch R., Heinrich G.: Morphology and fracture behaviour of polyethylene/Mg-Al layered double hydroxide (LDH) nanocomposites. European Polymer Journal, **42**, 2140-2152 (2006).
[192] Tjong S. C., Bao S. P.: Fracture toughness of high density polyethylene/SEBS-g-MA/montmorillonite nanocomposites. Composites Science and Technology, **67**, 314-323 (2007).
[193] Maspoch M. L., Franco-Urquiza E., Gamez-Perez J., Santana O. O., Sanchez-Soto M.: Fracture behaviour of poly[ethylene-(vinyl alcohol)]/organo-clay composites. Polymer International, **58**, 648-655 (2009).
[194] Ganss M., Satapathy B. K., Thunga M., Weidisch R., Potschke P., Jehnichen D.: Structural interpretations of deformation and fracture behavior of polypropylene/multi-walled carbon nanotube composites. Acta Materialia, **56**, 2247-2261 (2008).
[195] Satapathy B. K., Ganss M., Weidisch R., Potschke P., Jehnichen D., Keller T., Jandt K. D.: Ductile-to-semiductile transition in PP-MWNT nanocomposites. Macromolecular Rapid Communications, **28**, 834-841 (2007).
[196] Mouzakis D. E., Papanicolaou G. C., Argyrakis C., Kandilioti G., Kontarinis D., Gregoriou V. G.: Fracture toughness response and residual property modelling in polymer nanocomposites. Journal of Nanostructured Polymers and Nanocomposites, **4**, 100-109 (2008).
[197] Saminathan K., Selvakumar P., Bhatnagar N.: Fracture studies of polypropylene/nanoclay composite. Part 1: Effect of loading rates on essential work of fracture. Polymer Testing, **27**, 296-307 (2008).
[198] Bureau M. N., Perrin-Sarazin F., Ton-That M. T.: Polyolefin nanocomposites: Essential work of fracture analysis. Polymer Engineering and Science, **44**, 1142-1151 (2004).
[199] Bureau M. N., Ton-That M. T., Perrin-Sarazin F.: Essential work of fracture and failure mechanisms of polypropylene-clay nanocomposites. Engineering Fracture Mechanics, **73**, 2360-2374 (2006).
[200] Lim J. W., Hassan A., Rahmat A. R., Wahit M. U.: Mechanical behaviour and fracture toughness evaluation of rubber toughened polypropylene nanocomposites. Plastics Rubber and Composites, **35**, 37-46 (2006).
[201] Tjong S. C., Ruan Y. H.: Fracture behavior of thermoplastic polyolefin/clay nanocomposites. Journal of Applied Polymer Science, **110**, 864-871 (2008).
[202] Tjong S. C., Bao S. P., Hang G. D.: Polypropylene/montmorillonite nanocomposites toughened with SEBS-g-MA: Structure-property relationship. Journal of Polymer Science Part B-Polymer Physics, **43**, 3112-3126 (2005).

[203] Ahmad S. H., Rasid R., Surip S. N., Anuar H., Czigány T., Razak S. B. A.: Mechanical and fracture toughness behavior of TPNR nanocomposites. Journal of Composite Materials, **41**, 2147-2159 (2007).
[204] Lach R., Schneider K., Weidisch R., Janke A., Knoll K.: Application of the essential work of fracture concept to nanostructured polymer materials. European Polymer Journal, **41**, 383-392 (2005).
[205] Satapathy B. K., Lach R., Weidisch R., Schneider K., Janke A., Knoll K.: Morphology and crack toughness behaviour of nanostructured block copolymer/homopolyrner blends. Engineering Fracture Mechanics, **73**, 2399-2412 (2006).
[206] Chen N., Wan C. Y., Zhang Y., Zhang Y. X., Zhang C. M.: Fracture behavior of PVC/blendex/nano-$CaCO_3$ composites. Journal of Applied Polymer Science, **95**, 953-961 (2005).
[207] Qiao Y., Avlar S., Chakravarthula S. S.: Essential fracture work of nylon 6-silicate nanocomposites. Journal of Applied Polymer Science, **95**, 815-819 (2005).
[208] Yang J. L., Zhang Z., Zhang H.: The essential work of fracture of polyamide 66 filled with TiO2 nanoparticles. Composites Science and Technology, **65**, 2374-2379 (2005).
[209] Zhang H., Zhang Z., Yang J. L., Friedrich K.: Temperature dependence of crack initiation fracture toughness of various nanoparticles filled polyamide 66. Polymer, **47**, 679-689 (2006).
[210] Baldi F., Bignotti F., Tieghi G., Ricco T.: Rubber toughening of polyamide 6/organoclay nanocomposites obtained by melt blending. Journal of Applied Polymer Science, **99**, 3406-3416 (2006).
[211] Kobayashi H., Shioya M., Tanaka T., Irisawa T., Sakurai S., Yamamoto K.: Comparative study of fracture behavior between carbon black/poly(ethylene terephthalate) and multiwalled carbon nanotube/poly(ethylene terephthalate) composite films. Journal of Applied Polymer Science, **106**, 152-160 (2007).
[212] Garnier G., Chehab B., Yrieix B., Brechet Y., Flandin L.: On the essential work of fracture in polymer-metal multilayers. Journal of Materials Science, **44**, 5537-5543 (2009).
[213] Satapathy B. K., Weidisch R., Potschke P., Janke A.: Crack toughness behaviour of multiwalled carbon nanotube (MWNT)/polycarbonate nanocomposites. Macromolecular Rapid Communications, **26**, 1246-1252 (2005).
[214] Satapathy B. K., Weidisch R., Potschke P., Janke A.: Tough-to-brittle transition in multiwalled carbon nanotube (MWNT)/polycarbonate nanocomposites. Composites Science and Technology, **67**, 867-879 (2007).
[215] Wang Z. D., Lu J. J.: Essential and non-essential work of fracture of PI/SiO_2 hybrid thin films. Applied Composite Materials, **14**, 33-45 (2007).
[216] Ragosta G., Musto P., Abbate M., Russo P., Scarinzi G.: Fracture behaviour and deformation mechanisms of polyimide/silica hybrids. Macromolecular Symposia, **228**, 287-298 (2005).
[217] Ragosta G., Musto P.: Polyimide/silica hybrids via the sol-gel route: High performance materials for the new technological challenges. Express Polymer Letters, **3**, 413-428 (2009).
[218] Lauke B., Schuller T.: Essential work of interfacial fracture: a method to characterise adhesion at polymer-polymer interfaces. International Journal of Adhesion and Adhesives, **21**, 55-58 (2001).
[219] Haughie D. W., Buckley C. P., Wu J. J.: The integrity of welded interfaces in ultra-high molecular weight polyethylene: Part 2 - Interface toughness. Biomaterials, **27**, 3875-3881 (2006).
[220] Candal M. V., Gordillo A., Santana O. O., Sanchez J. J.: Study of the adhesion strength on overmoulded plastic materials using the essential work of interfacial fracture (EWIF) concept. Journal of Materials Science, **43**, 5052-5060 (2008).
[221] Vu-Khanh T.: The impact fracture of polymers: Unanswered questions. Trends in Polymer Science, **5**, 356-360 (1997).
[222] Bernal C. R., Frontini P. M.: Determination of fracture-toughness in rubber-modified glassy-polymers under impact conditions. Polymer Engineering and Science, **35**, 1705-1712 (1995).
[223] Gonzalez I., Eguiazabal J. I., Nazabal J.: On the use of the essential work of fracture procedure in the determination of the fracture energy of tough polymeric materials. Polymer Testing, **28**, 760-763 (2009).

[224] Vu-Khanh T.: Determination of the impact fracture parameters in ductile polymers. Polymer, **29**, 1979-1984 (1988).
[225] Vu-Khanh T.: Time-temperature dependence in fracture behavior of high impact polystyrene. Theoretical and Applied Fracture Mechanics, **29**, 75-83 (1998).
[226] Hourston D. J., Lane S., Zhang H. X.: Toughened thermoplastics: 2. Impact properties and fracture mechanisms of rubber modified poly(butylenes terephthalates). Polymer, **32**, 2215-2220 (1991).
[227] Wu J. S., Mai Y. W.: Ductile fracture and toughening mechanism in polymers. Materials Forum, **19**, 181-199 (1995).
[228] Huang J., Paul D. R.: Comparison of fracture behavior of nylon 6 versus an amorphous polyamide toughened with maleated poly(ethylene-1-octene) elastomers. Polymer, **47**, 3505-3519 (2006).
[229] Laura D. M., Keskkula H., Barlow J. W., Paul D. R.: Effect of glass fiber and maleated ethylene-propylene rubber content on the impact fracture parameters of nylon 6. Polymer, **42**, 6161-6172 (2001).
[230] Laura D. M., Keskkula H., Barlow J. W., Paul D. R.: Effect of rubber particle size and rubber type on the mechanical properties of glass fiber reinforced, rubber-toughened nylon 6. Polymer, **44**, 3347-3361 (2003).
[231] Okada O., Keskkula H., Paul D. R.: Fracture toughness of nylon-6 blends with maleated rubbers. Journal of Polymer Science Part B-Polymer Physics, **42**, 1739-1758 (2004).
[232] Pressly T. G., Keskkula H., Paul D. R.: Temperature dependence of the fracture behavior of nylon 6/ABS blends. Polymer, **42**, 3043-3055 (2001).
[233] Yoo Y. J., Shah R. K., Paul D. R.: Fracture behavior of nanocomposites based on poly (ethylene-co-methacrylic acid) ionomers. Polymer, **48**, 4867-4873 (2007).
[234] Karger-Kocsis J., Ferrer-Balas D.: On the plane-strain essential work of fracture of polymer sheets. Polymer Bulletin, **46**, 507-512 (2001).
[235] Gupta P., Wilkes G. L., Sukhadia A. M., Krishnaswamy R. K., Lamborn M. J., Wharry S. M., Tso C. C., DesLauriers P. J., Mansfield T., Beyer F. L.: Does the length of the short chain branch affect the mechanical properties of linear low density polyethylenes? An investigation based on films of copolymers of ethylene/1-butene, ethylene/1-hexene and ethylene/1-octene synthesized by a single site metallocene catalyst. Polymer, **46**, 8819-8837 (2005).
[236] Ching E. C. Y., Poon W. K. Y., Li R. K. Y., Mai Y. W.: Effect of strain rate on the fracture toughness of some ductile polymers using the essential work of fracture (EWF) approach. Polymer Engineering and Science, **40**, 2558-2568 (2000).
[237] Fasce L., Pettarin V., Bernal C., Frontini P.: Mechanical evaluation of propylene polymers under static and dynamic loading conditions. Journal of Applied Polymer Science, **74**, 2681-2693 (1999).
[238] Fasce L., Bernal C., Frontini P., Mai Y. W.: On the impact essential work of fracture of ductile polymers. Polymer Engineering and Science, **41**, 1-14 (2001).
[239] Pettarin V., Frontini P. M., Elicabe G. E.: Optimal ligament lengths in impact fracture toughness estimation by the essential work of fracture method. Polymer Testing, **24**, 189-196 (2005).
[240] Martinatti F., Ricco T.: High-rate fracture toughness evaluation by the 'J' integral approach and the method of the essential work of fracutre. in 'Impact and dynamic fracture of polymers and composites' eds.: Williams J. G. and Pavan A.) Impact and dynamic fracture of polymers and composites, London, 83-91 (1995)
[241] Santana O. O., Maspoch M. L., Martinez A. B.: Plane strain essential work of fracture in SENB geometry at low and high strain rates of PC/ABS blends. Polymer Bulletin, **39**, 511-518 (1997).
[242] Pegoretti A., Ricco T.: Rate and temperature effects on the plane stress essential work of fracture in semicrystalline PET. in 'Fracture of Polymers, Composites and Adhesives II,' eds.: Blackman B. R. K. and Pavan A. and Williams J. G.) Elsevier Ltd. and ESIS, Oxford, Vol 32, 89-100 (2003)
[243] Tjong S. C., Xu S. A., Mai Y. W.: Impact-specific essential work of fracture of maleic anhydride-compatibilized polypropylene/elastomer blends and their composites. Journal of Polymer Science Part B-Polymer Physics, **40**, 1881-1892 (2002).

[244] Chiou K. C., Chang F. C., Mai Y. W.: Impact specific essential work of fracture of compatibilized polyamide-6 (PA6)/poly(phenylene ether) (PPE) blends. Polymer Engineering and Science, **41**, 1007-1018 (2001).
[245] Ozkoc G., Bayram G., Bayramli E.: Impact essential work of fracture toughness of ABS/polyamide-6 blends compatibilized with olefin based copolymers. Journal of Materials Science, **43**, 2642-2652 (2008).
[246] Lievana E., Bernal C., Frontini P.: Essential work of fracture of rubber-modified polyamide 6 in impact. Polymer Engineering and Science, **44**, 1707-1715 (2004).
[247] Gonzalez I., Eguiazabal J. I., Nazabal J.: Characteristics of the brittle/tough transition of poly(butylene terephthalate)/maleinized poly(ethylene-octene) blends determined by the essential work of fracture procedure. Polymer Testing, **29**, 27-32 (2010).
[248] Tam W. Y., Cheung T. Y. H., Li R. K. Y.: Impact properties of glass fibre/impact modifier/polypropylene hybrid composites. Journal of Materials Science, **35**, 1525-1533 (2000).
[249] Bao S. P., Tjong S. C.: Impact essential work of fracture of polypropylene/montmorillonite nanocomposites toughened with SEBS-g-MA elastomer. Composites Part a-Applied Science and Manufacturing, **38**, 378-387 (2007).
[250] Tjong S. C., Xu S. A., Mai Y. W.: Drop weight impact and work of fracture of short glass fiber reinforced polypropylene composites toughened with elastomer. Polymer Composites, **24**, 437-447 (2003).
[251] Tjong S. C., Bao S. P.: Impact fracture toughness of polyamide-6/montmorillonite nanocomposites toughened with a maleated styrene/ethylene butylene/styrene elastomer. Journal of Polymer Science Part B-Polymer Physics, **43**, 585-595 (2005).
[252] Tjong S. C., Xu S. A., Mai Y. W.: Impact fracture toughness of short glass fiber-reinforced polyamide 6,6 hybrid composites containing elastomer particles using essential work of fracture concept. Materials Science and Engineering a-Structural Materials Properties Microstructure and Processing, **347**, 338-345 (2003).
[253] Yu H. Y., Zhang Y., Ren W. T.: Investigation on the fracture behavior and morphology of maleated poly(ethylene 1-octene) toughened and glass fiber-reinforced nylon 1010. Journal of Applied Polymer Science, **113**, 181-189 (2009).
[254] Kwon H. J., Jar P. Y. B.: Fracture toughness of polymers in shear mode. Polymer, **46**, 12480-12492 (2005).
[255] Kwon H. J., Jar P. Y. B.: Toughness of high-density polyethylene in shear fracture. International Journal of Fracture, **145**, 123-133 (2007).
[256] Chia J. Y. H., Cotterell B., Cheong A. Y. H.: The specific work of fracture in ball shear test and the integrity of solder balls. Materials Science and Engineering a-Structural Materials Properties Microstructure and Processing, **428**, 67-72 (2006).
[257] Rivlin R. S., Thomas A. G.: Rupture of Rubber. I. Characteristic energy for tearing. Journal of Polymer Science, **10**, 291-318 (1953).
[258] Wong J. S. S., Ferrer-Balas D., Li R. K. Y., Mai Y. W., Maspoch M. L., Sue H. J.: On tearing of ductile polymer films using the essential work of fracture (EWF) method. Acta Materialia, **51**, 4929-4938 (2003).
[259] Hashemi S.: Ductile fracture of polyester films. Plastics Rubber and Composites Processing and Applications, **20**, 229-237 (1993).
[260] Kuusipalo J., Huhtasalo L. J., Savijarvi A. M., Friend J. E., Mackerron D. H.: The influence of a multilayer structure on the fracture of polyester film. Journal of Materials Science, **41**, 301-304 (2006).
[261] Kuusipalo J., Savijarvi A. M., Norval S., Adlen M. J., Mackerron D. H.: The dependence of tear behaviour on the microstructure of biaxially drawn polyester film. Journal of Materials Science, **39**, 6909-6919 (2004).
[262] Kim H. S., Karger-Kocsis J.: Tearing resistance of some co-polyester sheets. Acta Materialia, **52**, 3123-3133 (2004).
[263] Yuan Y. L., Wu C. M. L., Li R. K. Y.: On the tearing fracture of polycarbonate films. Polymer Testing, **26**, 102-107 (2007).

[264] Wells A. A.: Application of fracture mechanics at and beyond general yielding. British Welding Journal, **10**, 563-570 (1963).
[265] Karac A., Ivankovic A.: Modelling the drop impact behaviour of fluid-filled polyethylene containers. in 'Fracture of Polymers, Composites and Adhesives II,' eds.: Blackman B. R. K. and Pavan A. and Williams J. G.) Elsevier Ltd. and ESIS, Oxford, Vol 32, 253-264 (2003)
[266] Kwon H. J., Jar P. Y. B.: New energy partitioning approach to the measurement of plane-strain fracture toughness of high-density polyethylene based on the concept of essential work of fracture. Engineering Fracture Mechanics, **74**, 2471-2480 (2007).
[267] Ben Jar P. Y., Adianto R.: Determination of Plane-Strain Fracture Toughness of Polyethylene Copolymer Based on the Concept of Essential Work of Fracture. Polymer Engineering and Science, **50**, 530-535 (2010).
[268] Ratna D., Karger-Kocsis J.: Recent advances in shape memory polymers and composites: a review. Journal of Materials Science, **43**, 254-269 (2008).
[269] Kim B. K.: Shape memory polymers and their future developments. Express Polymer Letters, **2**, 614-614 (2008).
[270] Karger-Kocsis J., Moskala E. J., Shang P. P.: Work of fracture and strain-induced cold crystallization behavior of amorphous copolyester sheets. Journal of Thermal Analysis and Calorimetry, **63**, 671-678 (2000).
[271] Karger-Kocsis J., Shang P. P., Moskala E. J.: Effects of deformation rate on the necking of an amorphous copolyester studied by modulated DSC. Journal of Thermal Analysis and Calorimetry, **55**, 21-28 (1999).
[272] Karger-Kocsis J.: Fracture mechanical behavior of thermoplastic polymers as a function of molecular and supermolecular variables. in 'The Application of Fracture Mechanics to Polymers, Adhesives and Composites' (ed.: Moore D. R.) Elsevier and ESIS Publ., Oxford, Vol 33, 25-29 (2004)
[273] Karger-Kocsis J.: Fracture and fatigue behavior of amorphous (co)polyesters as a function of molecular and network variables. in 'Handbook of Thermoplastic Polyesters' (ed.: Fakirov S.) Wiley-VCH, Weinheim, 717-753 (2002)
[274] Egan B. J., Delatycki O.: The morphology, chain structure and fracture-behavior of high-density polyethylene.1. Fracture at a constant rate of deflection. Journal of Materials Science, **30**, 3307-3318 (1995).
[275] Fayolle B., Audouin L., Verdu J.: Radiation induced embrittlement of PTFE. Polymer, **44**, 2773-2780 (2003).
[276] Duan K., Hu X. Z., Stachowiak G.: Modified essential work of fracture model for polymer fracture. Composites Science and Technology, **66**, 3172-3178 (2006).
[277] Drozdov A. D., Clyens S., Christiansen J.: Essential work of fracture and viscoplastic response of a carbon black-filled thermoplastic elastomer. Engineering Fracture Mechanics, **76**, 1977-1995 (2009).
[278] Cotterell B., Pardoen T., Atkins A. G.: Measuring toughness and the cohesive stress-displacement relationship by the essential work of fracture concept. Engineering Fracture Mechanics, **72**, 827-848 (2005).
[279] Naz S., Sweeney J., Coates P. D.: Analysis of the essential work of fracture method as applied to UHMWPE. Journal of Materials Science, **45**, 448-459 (2010).
[280] Korsunsky A. M., Kim K.: Determination of essential work of necking and tearing from a single tensile test. International Journal of Fracture, **132**, L37-L44 (2005).
[281] Korsunsky A. M., Nguyen G. D., Houlsby G. T.: Analysis of essential work of rupture using non-local damage-plasticity modelling. International Journal of Fracture, **135**, L19-L26 (2005).
[282] Korsunsky A. M., Nguyen G. D., Kim K.: The analysis of deformation size effects using multiple gauge length extensometry and the essential work of rupture concept. Materials Science and Engineering a-Structural Materials Properties Microstructure and Processing, **423**, 192-198 (2006).

[283] Karger-Kocsis J.: Dependence of the fracture and fatigue performance of polyolefins and related blends and composites on microstructural and molecular characteristics. Macromolecular Symposia, **143**, 185-205 (1999).
[284] Maier G. A., Wallner G., Lang R. W., Fratzl P.: Structural changes during plastic deformation at crack tips in PVDF films: A scanning X-ray scattering study. Macromolecules, **38**, 6099-6105 (2005).
[285] Riekel C., Karger-Kocsis J.: Structural investigation of the phase transformation in the plastic zone of a beta-phase isotactic polypropylene by synchrotron radiation microdiffraction. Polymer, **40**, 541-545 (1999).